The authors thank the editor and referees to review our manuscript and particularly for the valuable comments and suggestions that are very helpful in improving the manuscript. We provide below point-by-point responses to the referees' comments. We also have made most of the changes suggested by the referees in the revised manuscript.

Referee #1

The manuscript by Duan et al. reported atmospheric processes of secondary aerosols, including secondary inorganic and secondary organic aerosols in Beijing during summertime and wintertime. Although similar studies have been conducted in Beijing, there are some valuable information presented here. I agree with the reviewer 2 that the authors need to further highlight the novelty of this study in the revised manuscript.
Comments:
1. The authors resolved an isoprene-oxidized OA (ISOOA) in summer by using the constrained profile that was identified in southeastern US. I suggest the authors adding some discussions on the uncertainties in the text. ISOOA was generally formed in environment with low NOx and high biogenic emissions. Because the authors used ME2 for the source apportionment, any input spectral profile can force to separate an OA factor.

Response: We thank the referee's suggestion. It is indeed necessary to include some uncertainty estimation regarding the ISOOA factor. In our source apportionment using ME-2, the *a* value approach was used which determines the extent to which the output profiles can differ from the model inputs. We used high *a* values of 0.3-0.6 to constrain the ISOOA profile, allowing large variation of the ISOOA output profile. To further evaluate the uncertainties of this factor, we performed ME-2 with each *a* value (0.3-0.6) for 20 times and calculated the standard deviation of these solutions, which is now shown as the error bar in final ISOOA profile (Fig. S3). An uncertainty of ~20% was estimated for ISOOA in our measurement, suggesting a large uncertainty in ISOOA source in urban environment. The low mass fraction and concentration (5% of total OA and an average mass concentration of 1 μg m^{-3}) of this ISOOA factor may be another reason for the relatively high uncertainty.

In the revised supplementary page 2 line 7-14, we have now added the following discussion in source apportionment section:
"To minimize the bias from non-local input profiles, the *a* value approach was used which determines the extent to which the output profiles can differ from the model inputs. It should be particularly noted that we used high *a* values of 0.3-0.6 to constrain the ISOOA profile, allowing large variation of the ISOOA output profile. To further evaluate the uncertainties of this factor, we performed ME-2 with each *a* value (0.3-0.6) for 20 times and calculated the standard deviation of these solutions, which is shown as the error bar in final ISOOA profile (Fig. S3). An uncertainty of ~20% was estimated for ISOOA in our measurement, suggesting a large uncertainty in ISOOA source in urban environment."

In the revised manuscript page 7 line 1-7, we have now added the following discussion:
"…in summertime Beijing. ISOOA was generally thought to be formed in environment with low NOx and high biogenic emissions, but has recently been observed in urban Nanjing in

summer 2013 (Zhang et al., 2017). Similar to the result in summertime Nanjing (4% of OA), in our study ISOOA is found to contribute ~5% of total OA with an average mass concentration of 1.0 μg m^{-3} in summertime Beijing. In contrast, ISOOA was not resolved during winter, which is consistent with the low emissions of isoprene. It should be noted that the estimated uncertainty of ISOOA factor is ~20%, suggesting large uncertainty in ISOOA source in urban Beijing."

2. The authors claimed that aqueous-phase processed had significant impacts on the formation of sulfate in winter. According to the Figure 3b, the diurnal variations of SO4/CO was remarkably similar to that of NO3/CO. It seems that photochemical production was very important in winter, could the author give more explanations?

Response: We agree with the reviewer that photochemical oxidation also contributed to wintertime sulfate formation, as shown in Fig. S5h the sulfur oxidation ratio (SOR) in winter still displayed a positive correlation with Ox. However, it should be noted that the increasing rate of $SO_4^{2-}/\triangle CO$ was much lower than that of $NO_3^-/\triangle CO$ although their diurnal variations were similar. On the other hand, the exponential relationship between SOR and RH was much more obvious in winter than in summer (Fig. S5b and d), and the correlation between SO_4^{2-} and NO_3^- showed that higher concentrations of SO_4^{2-} were related to higher RH conditions in winter. Therefore, we concluded that aqueous-phase processes had relatively significant impacts on the formation of sulfate in winter.

In the revised manuscript page 10 line 11-20, we have now added the following discussion: "It is noted that the diurnal variations of $SO_4^{2-}/\triangle CO$ and $NO_3^-/\triangle CO$ were similar in winter (Fig. 3). However, the increasing rate of $SO_4^{2-}/\triangle CO$ was much lower than that of $NO_3^-/\triangle CO$. Also the absolute concentration of wintertime sulfate showed a decreasing trend in the afternoon, consistent with the diurnal variations of RH and ALWC, while the absolute concentration of wintertime nitrate showed an increasing trend from 8:00 to 18:00 LT (Fig. S4). These results further suggest the difference in dominant formation processes between sulfate and nitrate in winter. The photochemical processes were likely the dominant pathways for daytime nitrate formation but less important for sulfate formation because of large contributions from aqueous-phase processes as indicated by the exponential relationship between SOR and RH in wintertime Beijing (Fig. S5d)."

3. The color of OA factors in summer is difficult to read (e.g., Figure 1), suggesting the authors to change it.

Response: Change made. We have now changed the color of OOA in Figures 1, 2, 3, and 8 in the revised manuscript and Figures S3, S4 in the revised supplementary.

Referee #2

This manuscript reported the composition of submicron aerosol measured by an aerosol chemical speciation monitor (ACSM) in summer and winter in Beijing. PMF analysis is performed for the source apportionment of organic aerosol. Correlation analysis is used to investigate the formation mechanisms of nitrate, sulfate, and organic aerosol. The same measurements and data analysis have been repeatedly performed in Beijing as well as other megacities in China. This manuscript lacks novelty and in-depth discussions. Most of the conclusions are speculative. I am sorry that I cannot recommend publication in its current format.

Response: We agree with the referee that an increasing number of ACSM/AMS studies have been conducted in Beijing over the past few years. However, the causes of fine PM pollution in urban Beijing are still not fully understood, most likely due to the campaign-to-campaign difference in meteorological conditions, emissions, and atmospheric processes. In addition, previous studies conducted in different seasons usually focused on sources variations or only SIA or SOA formations (Sun et al., 2015; Hu et al., 2016; Hu et al., 2017; Xu et al., 2017). In our study, we present summer and winter measurements and discuss the seasonal difference in aerosol sources and secondary processes both on SIA and SOA formations. In particular, daytime oxidation formation efficiency of secondary aerosol during winter was found to be comparable to that during summer. Meanwhile, based on the correlation analysis with Ox and ALWC, diurnal variations of secondary species and evolutions from clean to pollution periods with different meteorological conditions between summer and winter, the relative importance of photochemistry versus aqueous-phase processes in the formation of both SIA and SOA were well investigated. Therefore, our study still provides valuable information to the scientific community to improve our understanding of fine PM pollution.

Major Comments

1. Page 6 Line 20-23. It is stated that the higher COA concentration in winter than summer suggests enhanced primary emission during winter. However, the changes are more likely caused by meteorological conditions than emissions, as the cooking activities are not expected to have seasonal variation.

Response: We agree with the reviewer. It now reads "COA also showed similar increasing trend from summer to winter, with mass concentration increasing from 3.4 μg m^{-3} to 6.3 μg m^{-3} and fractional contribution from 18% to 20%. The increase in mass concentration of COA in winter is likely caused by meteorological conditions (e.g., shallower PBL heights in winter than in summer) because the cooking activities are not expected to have seasonal variation."

2. Page 6 Line 24-26. In order to evaluate the effects of biomass burning control on air quality, the change in absolute BBOA concentration needs to be used, instead of the fraction of BBOA in total OA.

Response: Change made. It now reads "The average wintertime BBOA concentration decreased from 3.6 μg m^{-3} in 2010 (Hu et al., 2016) to 2.8 μg m^{-3} in 2015 in our study and further to 2.4 μg m^{-3} in 2017-2018 (Li et al., 2019), suggesting efficient control of the biomass burning activities in Beijing and surrounding areas in recent years.”

3. Page 6 Line 33-34. It is a bit surprising that two OOA factors are resolved in winter, but only one OOA factor is resolved in summer. This is different from the observation in Jimenez et al. 2009 Science and many others studies containing summer vs winter contrast. This doesn’t necessarily mean that the PMF results in this study are wrong, but it would be interesting to understand why. The instrument resolution is not the only reason, as it doesn’t change between seasons.

Response: This is a good question. In our study, two OOA factors (i.e., LO-OOA and MO-OOA) with much different time series were resolved in winter, and only one OOA factor was resolved in summer. When adding one more factor (i.e., from 4 factors to 5 factors) in the ME-2 model for summertime data, the additional factor is a split from the OOA factor according to the profile and time series (see the figure below). Actually, in some studies summarized in Jimenez et al. (2009), different OOA factors were resolved between summer and winter in the same measurement site using the same instrument. For example, only one OOA factor was resolved in winter and two OOA factors (i.e., SV-OOA and LV-OOA) were resolved in summer for the studies in Zurich (Lanz et al., 2007; 2008) and in Tokyo (Takegawa et al., 2005; 2006). Also the year-long measurement in Beijing conducted by Hu et al. (2017) resolved one OOA factor in spring and autumn, while two OOA factors including MO-OOA and LO-OOA in summer and winter.

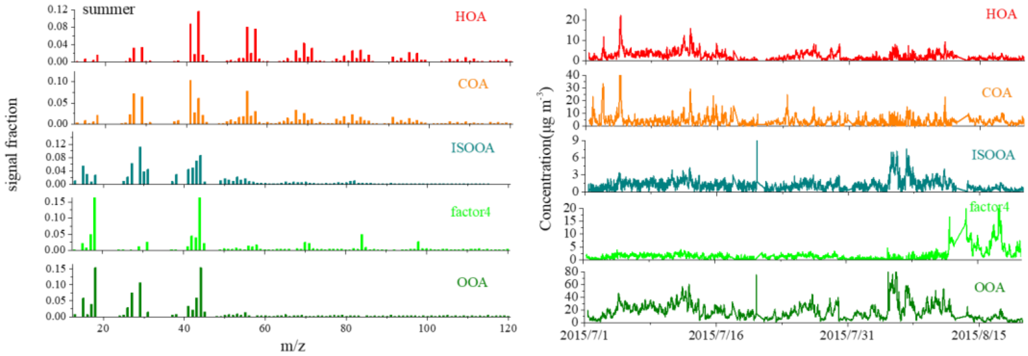

Figure 1. Mass spectrums (left) and time series (right) of OA sources for 5 factors solution during summer.

4. Page 8 Line 12-13. It is an interesting finding that “daytime oxidation formation efficiency of secondary aerosol during winter was comparable to that during summer”, but the reason for this observation warrants in-depth analysis. This is just one of many examples that can substantially improve the manuscript.

Response: We thank the referee’s suggestion. We note that wintertime photochemistry was traditionally thought to be low because the wintertime OH radical concentrations were traditionally thought to be low due to low O_3 concentrations (e.g., 9.2 ppb in winter versus 49.6 ppb in summer in our study) and reduced solar UV level in winter. However, recent measurements of OH radicals at a suburban site of Beijing reported wintertime OH radical concentrations at noontime ranged from 2.4×10^6 cm^{-3} in severely polluted air (k_{OH} ~27 s^{-1}) to 3.6×10^6 cm^{-3} in relatively clean air (k_{OH} ~5 s^{-1}) (Tan et al., 2018). These OH radical concentrations are nearly one order of magnitude larger than what global models predict for northern China in winter (Lelieveld et al., 2016). The higher-than-expected OH concentrations and moderate OH reactivity in Beijing resulted in fast photochemistry in winter (Lu et al., 2019), explaining the high contribution of secondary aerosol during wintertime severe haze events (Huang et al., 2014).

Regarding the sources of OH radicals, there have been increasing evidence showing HONO, instead of O_3, is the main source of OH radicals in wintertime North China Plain. Studies from four years of ground-based observations in urban Beijing and a nearby rural site (Xianghe) show that OH production from HONO photolysis is more than 10 times higher than that from O_3 photolysis in winter (Hendrick et al., 2014). Using the TUV radiation model, Xing et al. (2019) shows that in Beijing the estimated net OH production rate from HONO photolysis is 1.0×10^{-4} ppb s^{-1}, about 10 time higher than the estimated maximal OH production rate from O_3 photolysis (1.2×10^{-5} ppb s^{-1}). Further, Lu et al. (2019) found surprisingly high OH radical oxidation rates of up to 15 ppbv h^{-1} in Beijing in winter, which is comparable to that in summer and is mainly initiated by the photolysis of HONO and maintained by an extremely efficient radical cycling process driven by nitric oxide.

In the revised manuscript from page 8 line 35 to page 9 line 14, we have added the following discussion:
"Certainly, we note that wintertime photochemistry was traditionally thought to be low because the wintertime OH radical concentrations were traditionally thought to be low due to low O_3 concentrations (e.g., 9.2 ppb in winter versus 49.6 ppb in summer in our study) and reduced solar UV level in winter. However, recent measurements of OH radicals at a suburban site of Beijing reported wintertime OH radical concentrations at noontime ranged from 2.4×10^6 cm^{-3} during severe pollution events (k_{OH} ~27 s^{-1}) to 3.6×10^6 cm^{-3} during relatively clean events (k_{OH} ~5 s^{-1}) (Tan et al., 2018). These OH radical concentrations are nearly one order of magnitude larger than those predicted by global models for northern China in winter (Lelieveld et al., 2016). The higher-than-expected OH concentrations and moderate OH reactivity in Beijing resulted in fast photochemistry in winter (Lu et al., 2019), explaining the high contribution of secondary aerosol during wintertime severe haze events (Huang et al., 2014). Meanwhile, there have been increasing evidence showing HONO, instead of O_3, is the main source of OH radicals in wintertime North China Plain (Hendrick et al., 2014; Xing et al., 2019). Further, Lu et al. (2019) found surprisingly high OH radical oxidation rates of up to 15 ppbv h^{-1} in Beijing in winter, which is comparable to that in summer and is mainly initiated by the photolysis of HONO and maintained by an extremely efficient radical cycling process driven by nitric oxide."

5. Section 3.3. The rationale behind the scatter plot between NO3 and SO4 is not clear. NO3 and SO4 originates from different precursors, but this difference is ignored in the scatter plot. The conclusions from this analysis are also highly speculative. For example, the larger slope of NO3/SO4 is attributed to that high RH facilitates the gas/particle partitioning of

ammonium nitrate. However, wouldn't the high RH (or LWC to be more precise) have similar effect on ammonium sulfate? The formation of nitrate depends on many factors, including NOx, OH, temperature, RH (potentially), etc. The authors need to express more caution in interpreting the results from the simple correlation plots. The conclusions such as RH enhanced nitrate formation in summer and photochemical process dominating nitrate formation in winter are not well supported.

Response: Combining with the scatter plot between NO_3^- and SO_4^{2-}, we also discussed the effects of Ox and RH on SOR and NOR (see Fig. S5), which are related to the sulfate precursor SO_2 and nitrate precursor NO_2 respectively. Nitrate is a semi-volatile species whose formation can be affected by RH and temperature. High RH facilitates the gas-to-particle partitioning of ammonium nitrate. In comparison, sulfate is non-volatile and will stay in the particle phase. In addition, diurnal variations of SO_4^{2-} and NO_3^- and the evolution from clean days to pollution days with different meteorological conditions were also further used to support the conclusions, such as RH enhanced nitrate formation in summer and photochemical process dominated nitrate formation in winter. With information from these different aspects, we believe that it is a comprehensive analysis and provides valuable information on the formation of sulfate and nitrate.

6. Page 9 Line 17-18. It is written that "This suggests that RH has either no effects or complex effects on the OOA formation." This statement only illustrates that the previous analysis is not meaningful.

Response: We were trying to say that in summer photochemical oxidation was the dominant pathway for OOA formation, whereas contributions from aqueous-phase processes were minor and complex. For example, in the condition of low oxidation capacity (low O_x), high RH may facilitate the formation of OOA. We have made change and it now reads "This suggests that RH has relatively minor but complex effects on the formation of OOA during summer."

7. Section 3.4. Similar to the discussions on the formation mechanism of sulfate and nitrate, the effects of OA precursors are completely omitted in the discussion. Temperature is another important factor when contrasting the OA between summer and winter, but it is also ignored in the discussion.

Response: We agree with the referee that it will be very helpful for in-depth understanding of the SOA formation mechanisms through simultaneous measurements of particulate OA and its precursors (i.e., VOCs). However, in our study we focused on particle phase and did not measured VOCs and therefore could not link SOA with its VOCs. Nevertheless, Liu et al. (2018) measured VOCs in Beijing and found that high concentrations of VOC precursors might contribute to sustained organic aerosol growth and long duration of haze events under typical ambient conditions in Beijing.

Following the referee's suggestion, we have now discussed the effects of temperature on the formation of OOA. As shown in the figure below, both mass concentration and mass fraction of OOA showed positive correlations with temperature in summer, suggesting that high temperature promotes the oxidation and formation of OOA in summer. Further analysis shows a positive correlation between temperature and Ox ($R^2 = 0.59$) and a strong negative correlation between temperature and RH ($R^2 = 0.63$). This indicates that high temperature conditions in summer corresponded to high Ox and low RH conditions, further confirming the relatively important role of photochemical oxidation than aqueous-phase processes in the OOA formation during summer. In winter, however, both mass concentration and mass fraction of OOA (or LO-OOA and MO-OOA) showed no clear correlation with temperature. Also, there was no clear correlation between temperature and Ox or RH, suggesting a more complex effects of temperature on the SOA formation in winter.

In the revised supplement, we have now added the figure below as Figure S6, and in the revised manuscript page 11 line 2-13, we have added the following discussion:
"It should be noted that temperature could affect both atmospheric oxidative capacity and RH and therefore the photochemistry and aqueous-phase processes. As shown in Fig. S6, both mass concentration and mass fraction of OOA showed positive correlations with temperature, suggesting that high temarature promotes the oxidation and formation of OOA in summer. Further analysis shows a positive corralation between temparature and Ox ($R^2 = 0.59$) and a strong negative correlation between temperature and RH ($R^2 = 0.63$). This indicates that high temperature conditions in summer corresponded to high Ox and low RH conditions, further confirming the relatively important role of photochemical oxidation than aqueous-phase processes in the OOA formation during summer. In winter, however, both mass concentration and mass fraction of OOA (or LO-OOA and MO-OOA) showed no clear correlation with temperature. Also, there was no clear correlation between temperature and Ox or RH, suggesting a more complex effects of temperature on the SOA formation in winter."

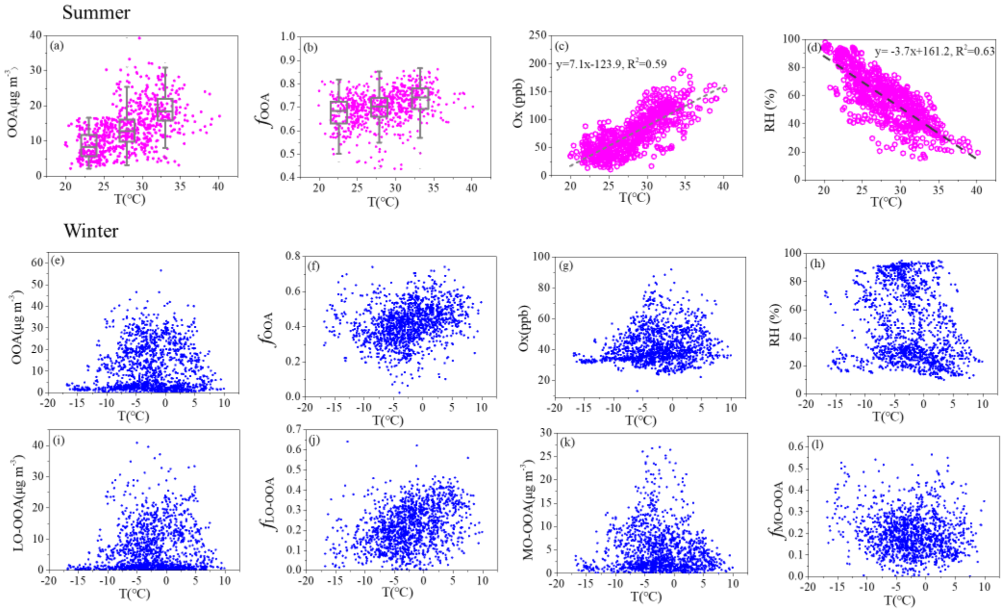

Figure 2. Effects of temperature on the formation of OOA in summer (a-d) and winter (e-l). OOA in winter refers to the sum of LO-OOA and MO-OOA.

Referee #3

This manuscript by Duan et al. presents measurement results in Beijing summer and winter with a focus on the secondary aerosol formation processes. The paper is overall written in fine English, and present results in a relatively clear way, but there remains some unresolved issues before its acceptance.

(1) A natural but critical question is novelty of the findings. The campaigns were conducted in 2015 (a bit old data), and a large number of AMS studies have been conducted in Beijing in recent years. Similar conclusions were already reported previously, for example the formation mechanisms of sulfate (and nitrate) in summer (photochemical dominant) and winter (aqueous processing dominant); the links between photochemical oxidation with LO-OOA and aq-processing with MO-OOA were also reported previously in Beijing (and some other cities); also, the methods used to conduct such analyses are also similar to prior studies. The authors must clearly state what new findings this paper can offer, and in the meantime, to highlight the differences of your results from previous ones (for instance, in Fig.2, you should also add results after 2015)

Response: We agree with the referee that an increasing number of AMS/ACSM studies have been conducted in Beijing over the past few years. However, the causes of fine PM pollution in urban Beijing are still not fully understood, most likely due to the campaign-to-campaign difference in meteorological conditions, emissions, and atmospheric processes. In addition, previous studies conducted in different seasons usually focused on sources variations or only SIA or SOA formations (Sun et al., 2015; Hu et al., 2016; Hu et al., 2017; Xu et al., 2017). In our study, we present summer and winter measurements and discuss the seasonal difference in aerosol sources and secondary processes both on SIA and SOA formations. In particular, we highlight that daytime oxidation formation efficiency of secondary aerosol during winter was comparable to that during summer. Meanwhile, based on the correlation analysis with Ox and ALWC, diurnal variations of secondary species and evolutions from clean to pollution periods with different meteorological conditions between summer and winter, the relative importance of photochemistry versus aqueous-phase processes in the formation of both SIA and SOA were well investigated. Therefore, our study still provides valuable information to the scientific community to improve our understanding of fine PM pollution.

Following the referee's suggestion, we have added results in Beijing after 2015 in the revised Fig. 2. In page 7 line 23-26, we have added "From summer 2015 to summer 2018, the PM_1 concentration continued decreasing while the SIA contribution was again higher than that during summer 2015 and the SOA faction was similar to that in summer 2015 (Zhou et al., 2019)."

In page 7 line 31-35, we have added "After 2015, the wintertime PM_1 concentration further decreased to 33.2 μg m^{-3} in 2017-2018 (Li et al., 2019), but showed a peak concentration (92.9 μg m^{-3}) in Nov-Dec 2016 because of prevailing air masses from south and northeast of Beijing and high frequencies of high RH and low wind speeds (Xu et al., 2018). Such changes again suggested that the difference in meteorological conditions is one of the major causes of severe particulate pollution in Beijing." and in line 38, we added

"However, from winter 2015 to 2018, the SIA fraction increased from 40% to 54%, suggesting the increased importance of SIA from 2015 to 2018."

(2) P2 Line 33-37. The aqueous formation of sulfate is indeed controversial, therefore I do not suggest the authors to make conclusions on it. For example, you state, "this pathway, has been ruled out*: : :*". This is still an open question in my opinion.

Response: Change made. It now reads "Moreover, the aqueous oxidation of SO_2 by NO_2 has been suggested to be an efficient pathway for sulfate formation (Cheng et al., 2016; Wang et al., 2016), although contribution from this pathway in real air is controversial and is still an open question (Guo et al., 2017; Liu et al., 2017)."

(3) I have a similar doubt with another reviewer regarding the PMF factors. The presence of ISOOA is in question. In urban environment of Beijing, even in summer, it is unlikely to have a significant biogenic SOA factor, this was very likely due to your initial input in ME-2. This is should be carefully checked. In addition, the terminology of different OA factors should be considered more carefully. As you used a Q-ACSM, which is unable to calculate the elemental ratios, how can you define a more (or less) oxidized OOA? If this is only based on the spectral characteristics or similarities with previously identified factors, you should state it clearly in your manuscript.

Response: We agree with the referee that biogenic SOA has minor contribution to OA in urban environment of Beijing. In our study, ISOOA contributed to only 5% of total OA (or average mass concentration of 1 μg m^{-3}). In our source apportionment using ME-2, the *a* value approach was used which determines the extent to which the output profiles can differ from the model inputs. We used high *a* values of 0.3-0.6 to constrain the ISOOA profile, allowing large variation of the ISOOA output profile. To further evaluate the uncertainties of this factor, we performed ME-2 with each *a* value (0.3-0.6) for 20 times and calculated the standard deviation of these solutions, which is now shown as the error bar in final ISOOA profile (Fig. S3). An uncertainty of ~20% was estimated for ISOOA in our measurement, suggesting a large uncertainty in ISOOA source in urban environment.

As for LO-OOA and MO-OOA factors, although no elemental ratios could be resolved in Q-ACSM, the difference in ratio of intensity at *m/z* 44 over that at *m/z* 43 ($f_{44/43}$) can be used to differentiate the oxidation state of OOA for UMR data (Ng et al., 2010). This method has been used in many ACSM studies (e.g., Sun et al., 2016, 2018; Wang et al., 2017; Xu et al., 2017). In our study, as shown in the supplement, two OOA factors with much different time series were resolved, and we defined one as more oxidized OOA (MO-OOA) and the other as less oxidized OOA(LO-OOA) because of much higher $f_{44/43}$ value of MO-OOA (8.6) than that of LO-OOA (2.6).

In the revised supplement page 2 line 7-14, we have now added the following discussion in source apportionment section:
"To minimize the bias from non-local input profiles, the *a* value approach was used which determines the extent to which the output profiles can differ from the model inputs. It

should be particularly noted that we used high *a* values of 0.3-0.6 to constrain the ISOOA profile, allowing large variation of the ISOOA output profile. To further evaluate the uncertainties of this factor, we performed ME-2 with each *a* value (0.3-0.6) for 20 times and calculated the standard deviation of these solutions, which is shown as the error bar in final ISOOA profile (Fig. S3). An uncertainty of ~20% was estimated for ISOOA in our measurement, suggesting a large uncertainty in ISOOA source in urban environment."

In the revised manuscript page 7 line 1-7, we have now added the following discussion: "…in summertime Beijing. ISOOA was generally thought to be formed in environment with low NOx and high biogenic emissions, but has recently been observed in urban Nanjing in summer 2013 (Zhang et al., 2017). Similar to the result in summertime Nanjing (4% of OA), in our study ISOOA is found to contribute ~5% of total OA with an average mass concentration of 1.0 μg m^{-3} in summertime Beijing. In contrast, ISOOA was not resolved during winter, which is consistent with the low emissions of isoprene. It should be noted that the estimated uncertainty of ISOOA factor is ~20%, suggesting large uncertainty in ISOOA source in urban Beijing."

In page 5 line 17-19, we have now added "Note that MO-OOA and LO-OOA were defined in winter because of much higher $f_{44/43}$ value of MO-OOA (8.6) than that of LO-OOA (2.6) and the large difference in time series of these two factors."

(4) In Figures 4 and 5, it is better to show the correlation coefficients.

Response: Thanks for the suggestion. In Fig. 4, we investigated the effects of RH and Ox on the relationship between SO_4^{2-} and NO_3^- and thus did not show the correlation coefficients. Actually, there was a good correlation between SO_4^{2-} and NO_3^- in winter with R^2 value of 0.67, while the correlation between SO_4^{2-} and NO_3^- was weak for all data in summer (R^2=0.13). In Fig. 5, the data points are rather scattering and thus we used box plots to see the trends for some figures. Generally, these two figures show the general trends and thus we did not show the correlation coefficients.

(5) Some researchers argue that ALWC and Ox may not be effective indicators for aqueous processing and photochemical processing, even though a few studies conducted similar analyses. There could be large uncertainties, and the data are also of large scatter, therefore complicates interpretation of your results. Such uncertainties should be discussed.

Response: We agree with the referee that there are uncertainties when using ALWC and Ox as indicator to investigate the aqueous-phase processes and photochemical processes. Therefore, more studies and sophisticated instruments are required to find out more effective indicators for aqueous-phase and photochemical processes of SOA. For example, the measurements of OH radicals to replace Ox could be more effective for investigating the atmospheric oxidative capacity. We have added the following uncertainty statement as a caution in the revised manuscript page 10 line 22-25:
"It should be note that a majority of the data are scattering, therefore caution should be

given for the uncertainties when using O_x and ALWC as indicators of photochemical processing and aqueous processing, respectively."

(6) Other influencing factors should also be considered when you look into the correlation of OOA factors with ALWC or Ox. For example, you tried to minimize the influence of PBL height by using delta CO; such influences from weather conditions rather than chemistry itself may also affect your analyses here. How about you investigate correlation of OOA/delta CO with ALWC, for example? In addition, I also suggest to discuss influences of different air masses on the correlations.

Response: We agree with the referee that the formation of OOA is affected by many factors including chemical, physical and meteorological factors. The complexity in OOA formation and the campaign-to-campaign difference are the main motivation of our study. When investigating the effects of Ox and ALWC on OOA formation, we have actually shown both absolute mass concentration and mass fraction of OOA (see Fig. 5 and 6). The mass fraction of OOA (f_{OOA}, $f_{\mathrm{LO\text{-}OOA}}$, or $f_{\mathrm{MO\text{-}OOA}}$) is actually a value normalized to total OA, and therefore can minimize the influence of PBL (similar to those normalized to delta CO).
Following the referee's suggestion, we have further investigated the influences of different air masses on the correlations (see the figures below). The cluster analysis results show 5 clusters of air masses in summer and 3 clusters of air masses in winter. However, there were no significant differences in these correlations for different air masses in both summer and wither.

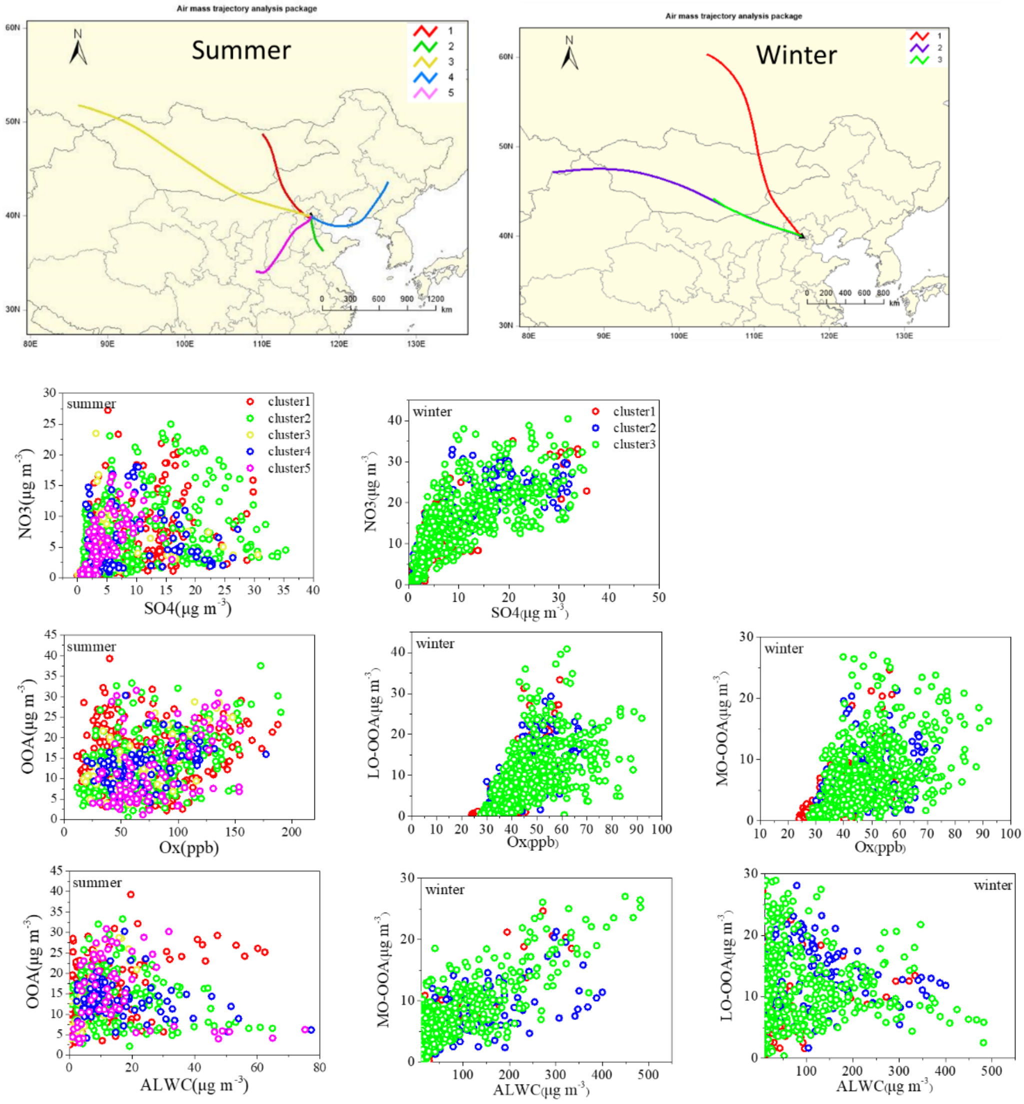

Figure 3. Influences of different air masses on the correlations between SO4 and NO3, as well as OOA and Ox or ALWC during summer and winter.

References:

Cheng, Y. F., Zheng, G. J., Wei, C., Mu, Q., Zheng, B., Wang, Z. B., Gao, M., Zhang, Q., He, K. B., Carmichael, G., Pöschl, U., and Su, H.: Reactive nitrogen chemistry in aerosol water as a source of sulfate during haze events in China, Science Advances, 2(12), e1601530, https://doi.org/10.1126/sciadv.1601530, 2016.

Guo, H., Weber, R. J., Nenes, A.: High levels of ammonia do not raise fine particle pH sufficiently to yield nitrogen oxide-dominated sulfate production, Sci. Rep., 7(1), 12109, 2017.

Hendrick, F., Müller, J. F., Clémer, K., Wang, P., De Mazière, M., Fayt, C., Gielen, C., Hermans, C., Ma, J. Z., Pinardi, G., Stavrakou, T., Vlemmix, T., and Van Roozendael, M.: Four years of ground-based MAX-DOAS observations of HONO and NO2 in the Beijing area, Atmos.

Chem. Phys., 14, 765–781, 2014.

Hu, W., Hu, M., Hu, W., Jimenez, J. L., Yuan, B., Chen, W., Wang, M., Wu, Y., Chen, C., Wang, Z., Peng, J., Zeng, L., and Shao, M.: Chemical composition, sources, and aging process of submicron aerosols in Beijing: Contrast between summer and winter, J. Geophys. Res. Atmos., 121(4), 1955–1977, https://doi.org/10.1002/2015JD024020, 2016.

Hu, W., Hu, M., Hu, W.-W., Zheng, J., Chen, C., Wu, Y., and Guo, S.: Seasonal variations in high time-resolved chemical compositions, sources, and evolution of atmospheric submicron aerosols in the megacity Beijing, Atmos. Chem. Phys., 17, 9979–10000, https://doi.org/10.5194/acp-17-9979-2017, 2017.

Huang, R. J., Zhang, Y. L., Bozzetti, C., Ho, K. F., Cao, J. J., Han, Y. M., Daellenbach, K. R., Slowik, J. G., Platt, S. M., Canonaco, F., Zotter, P., Wolf, R., Pieber, S. M., Bruns, E. A., Crippa, M., Ciarelli, G., Piazzalunga, A., Schwikowski, M., Abbaszade, G., Schnelle-Kreis, J., Zimmermann, R., An, Z., Szidat, S., Baltensperger, U., Haddad, I.E., and Prevot, A.S.H.: High secondary aerosol contribution to particulate pollution during haze events in China, Nature, 514, 218–222, 2014.

Jimenez, J. L., Canagaratna, M. R., Donahue, N. M., Prevot, A. S. H., Zhang, Q., Kroll, J. H., DeCarlo, P. F., Allan, J. D., Coe, H., Ng, N. L., Aiken, A. C., Docherty, K. S., Ulbrich, I. M., Grieshop, A. P., Robinson, A. L., Duplissy, J., Smith, J. D., Wilson, K. R., Lanz, V. A., Hueglin, C., Sun, Y. L., Tian, J., Laaksonen, A., Raatikainen, T., Rautiainen, J., Vaattovaara, P., Ehn, M., Kulmala, M., Tomlinson, J. M., Collins, D. R., Cubison, M. J., E, Dunlea, J., Huffman, J. A., Onasch, T. B., Alfarra, M. R., Williams, P. I., Bower, K., Kondo, Y., Schneider, J., Drewnick, F., Borrmann, S., Weimer, S., Demerjian, K., Salcedo, D., Cottrell, L., Griffin, R., Takami, A., Miyoshi, T., Hatakeyama, S., Shimono, A., Sun, J. Y., Zhang, Y. M., Dzepina, K., Kimmel, J. R., Sueper, D., Jayne, J. T., Herndon, S. C., Trimborn, A. M., Williams, L. R., Wood, E. C., Middlebrook, A. M., Kolb, C. E., Baltensperger, U., and Worsnop, D. R.: Evolution of organic aerosols in the atmosphere, Science, 326, 1525–1529, doi:10.1126/science.1180353, 2009.

Lanz, V. A., Alfarra, M. R., Baltensperger, U., Buchmann, B., Hueglin, C., and Prévôt, A. S. H.: Source apportionment of submicron organic aerosols at an urban site by factor analytical modelling of aerosol mass spectra, Atmos. Chem. Phys., 7, 1503–1522, https://doi.org/10.5194/acp-7-1503-2007, 2007.

Lanz, V. A., Alfarra, M. R., Baltensperger, U., Buchmann, B., Hueglin, C., Szidat, S., Wehrli, M. N., Wacker, L., Weimer, S., Caseiro, A., Puxbaum, H., and Prévôt, A. S. H.: Source attribution of submicron organic aerosols during wintertime inversions by advanced factor analysis of aerosol mass spectra, Environ. Sci. Technol., 42(1), 214-220,2008.

Lelieveld, J., Gromov, S., Pozzer, A., and Taraborrelli, D.: Global tropospheric hydroxyl distribution, budget and reactivity, Atmos. Chem. Phys., 16, 12477–12493, https://doi.org/10.5194/acp-16-12477-2016, 2016.

Li, H., Cheng, J., Zhang, Q., Zheng, B., Zhang, Y., Zheng, G., and He, K.: Rapid transition in winter aerosol composition in Beijing from 2014 to 2017: response to clean air actions, Atmos. Chem. Phys., 19, 11485–11499, https://doi.org/10.5194/acp-19-11485-2019, 2019.

Liu, J., Chu, B., Chen, T., Liu, C., Wang, L., Bao, X., and He, H.: Secondary organic aerosol formation from ambient air at an urban site in Beijing: effects of OH exposure and precursor concentrations. Environ. Sci. Technol., 52(12), 6834-6841, 2018.

Liu, M., Song, Y., Zhou, T., Xu, Z., Yan, C., Zheng, M., Wu, Z., Hu, M., Wu, Y., and Zhu, T.: Fine particle pH during severe haze episodes in northern China, Geophys. Res. Lett., 44(10), 5213-5221, 2017.

Lu, K., Fuchs, H., Hofzumahaus, A., Tan, Z., Wang, H., Zhang, L., Schmitt, S., Rohrer, F., Bohn, B., Broch, S., Dong, H., Gkatzelis, G., Hohaus, T., Holland, F., Li, X., Liu, Y., Liu, Y. H., Ma, X., Novell, A., Schlag, P., Shao, M., Wu, Y., Wu, Z., Zeng, L., Hu, M., Kiendler-Scharr, A., Wahner, A., and Zhang, Y.: Fast Photochemistry in Wintertime Haze: Consequences for Pollution Mitigation Strategies, Environ. Sci. Technol., 53(18), 10676-10684, 2019.

Ng, N. L., Canagaratna, M. R., Zhang, Q., Jimenez, J. L., Tian, J., Ulbrich, I. M., Kroll, J. H., Docherty, K. S., Chhabra, P. S., Bahreini, R., Murphy, S. M., Seinfeld, J. H., Hildebrandt, L., Donahue, N. M., DeCarlo, P. F., Lanz, V. A., Prévôt, A. S. H., Dinar, E., Rudich, Y., and Worsnop, D. R.: Organic aerosol components observed in Northern Hemispheric datasets from Aerosol Mass Spectrometry, Atmos. Chem. Phys., 10, 4625–4641, https://doi.org/10.5194/acp-10-4625-2010, 2010.

Sun, Y. L., Wang, Z. F., Du, W., Zhang, Q., Wang, Q. Q., Fu, P. Q., Pan, X., Li, J., Jayne, J., and Worsnop, D. R.: Long-term real-time measurements of aerosol particle composition in Beijing, China: seasonal variations, meteorological effects, and source analysis, Atmos. Chem. Phys., 15, 10149–10165, https://doi.org/10.5194/acp-15-10149-2015, 2015.

Sun, Y., Chen, C., Zhang, Y., Xu, W., Zhou, L., Cheng, X., Zheng, H., Ji, D., Li, J., Tang, X., Fu, P., and Wang, Z.: Rapid formation and evolution of an extreme haze episode in Northern China during winter 2015, Sci. Rep., 6(1), 1-9, 2016.

Sun, Y., Xu, W., Zhang, Q., Jiang, Q., Canonaco, F., Prévôt, A. S., Fu, P., Li, J., Jayne, J., Worsnop, D. R., and Wang, Z.: Source apportionment of organic aerosol from two-year highly time-resolved measurements by an aerosol chemical speciation monitor in Beijing, China, Atmos. Chem. Phys., 18(12), 8469–8489, 2018.

Takegawa, N., Miyazaki, Y., Kondo, Y., Komazaki, Y., Miyakawa, T., Jimenez, J. L., Jayne, J. T., Worsnop, D. R., Allan, J. D., and Weber, R. J.: Characterization of an Aerodyne Aerosol Mass Spectrometer (AMS): Intercomparison with other aerosol instruments, Aerosol Sci. Tech., 39(8), 760-770, 2005.

Takegawa, N., Miyakawa, T., Kondo, Y., Jimenez, J. L., Zhang, Q., Worsnop, D. R., and Fukuda, M.: Seasonal and diurnal variations of submicron organic aerosol in Tokyo observed using the Aerodyne aerosol mass spectrometer, J. Geophys. Res. Atmos., 111(D11), 2006.

Tan, Z., Rohrer, F., Lu, K., Ma, X., Bohn, B., Broch, S., Dong, H., Fuchs, H., Gkatzelis, G. I., Hofzumahaus, A., Holland, F., Li, X., Liu, Y., Liu, Y., Novelli, A., Shao, M., Wang, H., Wu, Y., Zeng, L., Hu, M., Kiendler-Scharr, A., Wahner, A., and Zhang, Y.: Wintertime photochemistry in Beijing: observations of ROx radical concentrations in the North China Plain during the BEST-ONE campaign, Atmos. Chem. Phys., 18, 12391–12411, https://doi.org/10.5194/acp-18-12391-2018, 2018.

Wang, G. H., Zhang, R. Y., Gomez, M. E., Yang, L. X., Zamora, M. L., Hu, M., Lin, Y., Peng, J. F., Guo, S., Meng, J. J., Li, J. J., Cheng, C. L., Hu, T. F., Ren, Y. Q., Wang, Y. S., Gao, J., Cao, J. J., An, Z. S., Zhou, W. J., Li, G. H., Wang, J. Y., Tian, P. F., Marrero-Ortiz, W., Secrest, J., Du, Z. F., Zheng, J., Shang, D. J., Zeng, L. M., Shao, M., Wang, W. G., Huang, Y., Wang, Y., Zhu, Y. J., Li, Y. X., Hu, J. X., Pan, B., Cai, L., Cheng, Y. T., Ji, Y. M., Zhang, F., Rosenfeld, D., Liss, P. S., Duce, R. A., Kolb, C. E., and Molina, M. J.: Persistent sulfate formation from London Fog to Chinese haze, Proc. Natl. Acad. Sci. U.S.A., 113(48), 13630–13635, 2016.

Wang, Y. C., Huang, R. J., Ni, H. Y., Chen, Y., Wang, Q. Y., Li, G. H., Tie, X. X., Shen, Z. X., Huang, Y., Liu, S. X., Dong, W. M., Xue, P., Fröhlich, R., Canonaco, F., Elser, M., Daellenbach, K.R., Bozzetti, C., Haddad, EI., and Cao, J. J.: Chemical composition, sources and secondary processes of aerosols in Baoji city of northwest China, Atmos. Environ., 158, 128–137, https://doi.org/10.1016/j.atmosenv.2017.03.026, 2017.

Xing, L., Wu, J., Elser, M., Tong, S., Liu, S., Li, X., Liu, L., Cao, J., Zhou, J., El-Haddad, I., Huang, R., Ge, M., Tie, X., Prévôt, A. S. H., and Li, G.: Wintertime secondary organic aerosol formation in Beijing–Tianjin–Hebei (BTH): contributions of HONO sources and heterogeneous reactions, Atmos. Chem. Phys., 19, 2343–2359, https://doi.org/10.5194/acp-19-2343-2019, 2019.

Xu, W. Q., Han, T. T., Du, W., Wang, Q. Q., Chen, C., Zhao, J., Zhang, Y. J., Li, J., Fu, P. Q., Wang, Z. F., Worsnop, D. R., and Sun, Y. L.: Effects of Aqueous-Phase and Photochemical Processing on Secondary Organic Aerosol Formation and Evolution in Beijing, China, Environ. Sci. Technol., 51(2), 762–770, https://doi.org/10.1021/acs.est.6b04498, 2017.

Xu, W. Q., Sun, Y. L., Wang, Q. Q., Zhao, J., Wang, J. F., Ge, X. L., Xie, C. H., Zhou, W., Du, W., Li, J., Fu, P. Q., Wang, Z. F., Worsnop, D. R., and Coe, H.: Changes in aerosol chemistry from 2014 to 2016 in winter in Beijing: insights from high resolution aerosol mass spectrometry, J. Geophys. Res. Atmos., 124(2), 1132–1147, 2018.

Zhang, Y. J., Tang, L. L., Sun, Y. L., Favez, O., Canonaco, F., Albinet, A., Couvidat, F., Liu, D. T., Jayne, J. T., Wang, Z., Croteau, P. L., Canagaratna, M. R., Zhou, H. C., Prevot, A. S. H., and Worsnop, D.R.: Limited formation of isoprene epoxydiols-derived secondary organic aerosol under NOx-rich environments in Eastern China, Geophys. Res. Lett., 44(4), 2035–2043, https://doi.org/10.1002/2016GL072368, 2017.

Zhou, W., Gao, M., He, Y., Wang, Q., Xie, C., Xu, W., Zhao, J., Du, W., Qiu, Y., Lei, L., Fu, P., Wang, Z., Worsnop, D.R., Zhang, Q., and Sun, Y.: Response of aerosol chemistry to clean air action in Beijing, China: Insights from two-year ACSM measurements and model simulations, Environ. Pollut., 255, 113345, 2019.

Summertime and wintertime atmospheric processes of secondary aerosol in Beijing

Jing Duan[1,2,3], Ru-Jin Huang[1,2], Yongjie Li[4], Qi Chen[5], Yan Zheng[5], Yang Chen[6], Chunshui Lin[1,2], Haiyan Ni[1,2], Meng Wang[1,2], Jurgita Ovadnevaite[7], Darius Ceburnis[7], Chunying Chen[8], Douglas R. Worsnop[9], Thorsten Hoffmann[10], Colin O'Dowd[7], Junji Cao[1,2]

[1]State Key Laboratory of Loess and Quaternary Geology (SKLLQG) and Key Laboratory of Aerosol Chemistry & Physics (KLACP), Institute of Earth Environment, Chinese Academy of Sciences, Xi'an 710061, China

[2]CAS Center for Excellence in Quaternary Science and Global Change, Chinese Academy of Sciences, Xi'an 710061, China

[3]University of Chinese Academy of Sciences, Beijing 100049, China

[4]Department of Civil and Environmental Engineering, Faculty of Science and Technology, University of Macau, Taipa, Macau 999078, China

[5]State Key Joint Laboratory of Environmental Simulation and Pollution Control, College of Environmental Sciences and Engineering, Peking University, Beijing 100871, China

[6]Chongqing Institute of Green and Intelligent Technology, Chinese Academy of Sciences, Chongqing 400714, China

[7]School of Physics and Centre for Climate and Air Pollution Studies, Ryan Institute, National University of Ireland Galway, University Road, Galway, H91CF50, Ireland

[8]CAS Key Laboratory for Biological Effects of Nanomaterials and Nanosafety, National Centre for Nanoscience and Technology, Beijing 100191, China

[9]Aerodyne Research, Inc., Billerica, MA, USA

[10]Institute of Inorganic and Analytical Chemistry, Johannes Gutenberg University Mainz, Duesbergweg 10–14, Mainz 55128, Germany

Correspondence to: Ru-Jin Huang (rujin.huang@ieecas.cn) or Qi Chen (qichenpku@pku.edu.cn)

Abstract

Secondary aerosol constitutes a large fraction of fine particles in urban air of China. However, its formation mechanisms and atmospheric processes remain largely uncertain despite considerable studies in recent years. To elucidate the seasonal variations of fine particles composition and secondary aerosol formation, an Aerodyne quadrupole aerosol chemical speciation monitor (Q-ACSM) combined with other online instruments were used to characterize the submicron particulate matter (diameter < 1 μm, PM_1) in Beijing during summer and winter 2015. Our results suggest that the photochemical oxidation was the major pathway for sulfate formation during summer, whereas aqueous-phase reaction became an important process for sulfate formation during winter. High concentration of nitrate (17% of the PM_1 mass) was found during winter explained by enhanced gas-to-particle partitioning at low temperature, while high nitrate concentration (19%) was also observed under the conditions of high relative humidity (RH) during summer likely due to the hydrophilic property of NH_4NO_3 and hydrolysis of N_2O_5. As for organic aerosol (OA) sources, secondary OA (SOA) dominated the OA mass (74%) during summer while the SOA contribution decreased to 39% during winter due to enhanced primary emissions in the heating season. In terms of the SOA formation, photochemical oxidation perhaps played an important role for summertime oxygenated OA (OOA) formation and wintertime less oxidized OOA (LO-OOA) formation. The wintertime more oxidized OOA (MO-OOA) showed a good correlation with aerosol liquid water content (ALWC), indicating more important contribution of aqueous-phase processing than photochemical production to MO-OOA. Meanwhile, the dependence of LO-OOA and the mass ratio of LO-OOA to MO-OOA on atmospheric oxidative tracer (i.e., O_x) both degraded when RH were greater than 60%, suggesting that RH or aerosol liquid water may also affect the LO-OOA formation.

1. Introduction

Haze pollution in the North China Plain (NCP) occurs in all seasons and is characterized by high concentrations of fine particulate matter (PM) (Huang et al., 2014; Yang et al., 2015; An et al., 2019). The haze episodes have become more frequent and severe in recent years, although the annual average concentration of $PM_{2.5}$ (aerodynamic diameter ≤ 2.5 μm) in the NCP has decreased due to the implementation of a variety of regulatory measures (Fontes et al., 2017; Sun et al., 2016; Xu et al., 2018). A better understanding of the chemical nature, formation and transformation of fine particles is therefore essential for mitigating the haze pollution.

Compared to primary aerosol that is relatively well constrained in terms of the emission sources, secondary aerosol is still not well understood, likely due to its variable precursors, complex formation and atmospheric transformation processes mediated by meteorological conditions (Ding et al., 2016; Petäjä et al., 2016; Tie et al., 2017; Xu et al., 2017). A number of studies have investigated the formation and aging processes of secondary aerosol (Takegawa et al., 2009; Huang et al., 2014, 2019; Sun et al., 2014, 2016; Cheng et al., 2016; Wang et al., 2016; Duan et al., 2019). For example, field measurements showed that aqueous-phase oxidation of SO_2 could be an important formation pathway of sulfate at high RH during haze events (Sun et al., 2014; Elser et al., 2016). Our recent study, however, suggested that the role of photochemical oxidation versus aqueous-phase reactions in the sulfate formation largely depends on the meteorological conditions (Duan et al., 2019). ~~Moreover, the aqueous oxidation of SO_2 by NO_2 has been suggested to be an efficient pathway for sulfate formation (Cheng et al., 2016; Wang et al., 2016). This pathway, however, has been ruled out because the particles are mostly acidic even at high NH_3 level as is estimated by Guo et al. (2017) and Liu et al. (2017).~~ Moreover, the aqueous oxidation of SO_2 by NO_2 has been suggested to be an efficient pathway for sulfate formation (Cheng et al., 2016; Wang et al., 2016), although contribution from this pathway in real air is controversial and is still an open question (Guo et al., 2017; Liu et al., 2017). Model simulation has showed that heterogeneous sulfate formation from SO_2 oxidation catalyzed by Fe^{3+} in aerosol water can significantly improve the sulfate simulation (Li et al., 2017). These studies show that even for sulfate, a simple inorganic component, the formation is complex during haze events. As for secondary organic aerosol (SOA), the formation pathways are much less understood given the complexity in SOA composition and its precursors. The contribution of SOA to $PM_{2.5}$ mass was found to be as important as secondary inorganic aerosol (SIA-sulfate, nitrate and ammonium) during severe haze events (Huang et al., 2014). Positive matrix factorization (PMF) analyses have resolved multiple OA factors. In particular, photochemical oxidation has been suggested to be the major pathway of SOA formation during some pollution events in some cities (e.g., Beijing and Xi'an) because SOA correlated tightly with odd oxygen (O_x) and was independent of RH (e.g., Sun et al., 2014; Elser et al., 2016). However, aqueous-phase formation of SOA has also been considered as an important pathway during some pollution events in e.g., Beijing, Shijiazhuang and Baoji (Sun et al., 2016; Wang et al., 2017; Huang et al., 2019). The formation of less oxidized oxygenated OA (LO-OOA) and more oxidized oxygenated OA(MO-OOA) in Baoji seemed being significantly influenced by aqueous-phase chemistry during the period of low atmospheric oxidative capacity (Wang et al., 2017), while in another study Xu et al. (2017) suggested that aqueous-phase processing has a dominant impact on the MO-OOA formation but photochemical oxidation is the dominant pathway for the LO-OOA formation in Beijing. It is unclear yet whether the aqueous-phase processing plays a key role in the haze development and what the mechanisms are.

Based on previous studies, it is evident that the formation of secondary aerosol shows large spatial and temporal variations and may vary in different events especially for the SOA formation. Further studies are therefore needed to better understand the formation and transformation of secondary aerosol in polluted air. As the pollutant emissions, meteorological conditions and oxidation capacity vary dramatically between summer and winter, in order to further elucidate the atmospheric processes of secondary aerosol under distinctly different atmospheric conditions, here we present results from summertime and wintertime measurements in 2015 in Beijing. The seasonal difference in aerosol chemical composition and in formation mechanisms are discussed.

2. Experimental

2.1 Measurement site

The summer (1 July to 19 August 2015) and winter (4 December 2015 to 6 February 2016) campaigns were conducted at an urban site on the roof of a five-story building (~20 m above the ground) in the National Center for Nanoscience (39.99°N, 116.32°E) in Beijing, which is close to the fourth ring of Beijing and surrounded by residential, commercial and traffic areas.

2.2 Instrumentation

An Aerodyne quadrupole ACSM (Q-ACSM) with a time resolution of ~30 min was deployed for the continuous measurement of NR-PM_1 species including organics, sulfate, nitrate, ammonium and chloride. Detailed operation principles of ACSM can be found elsewhere (Ng et al., 2011; Wang et al., 2017; Duan et al., 2019). Briefly, ambient air was sampled through a 3/8 inch stainless steel tube at a flow rate of ~3 L min^{-1}, and the coarse particles were removed by an Uuniversity Research Glassware (URG) cyclone (Model: URG-2000-30ED) with a size cut of 2.5 μm in front of the sampling inlet. A Nafion dryer (MD-110-48S, Perma Pure, Inc., Lakewood, NJ, USA) was applied to dry aerosol particles before entering the ACSM and the submicron aerosol was subsampled into the ACSM at a flow rate of 85 mL min^{-1} through a 100 μm diameter critical aperture. The submicron particles were focused into a narrow beam by an aerodynamic lens and impacted a hot vaporizer (~600℃). The resulting vapor was ionized with electron impact (70 eV) and chemically characterized with a quadrupole mass spectrometer. Mono-dispersed 300 nm ammonium nitrate particles, generated by an atomizer (Model 9302, TSI Inc., Shoreview, MN, USA) and selected by a differential mobility analyzer (DMA, TSI model 3080), were used to determine the response factor (RF) and calibrate the ionization efficiency (IE) for the ACSM (Ng et al., 2011).

An Aethalometer (Model AE-33, Magee Scientific) was used for the determination of equivalent black carbon (eBC) concentration with a time resolution of 1 min. SO_2, CO, NO_x and O_3 were measured by an Ecotech EC 9850 sulfur dioxide analyzer, a Thermo Scientific Model 48i carbon monoxide analyzer, a Thermo Scientific Model 42i NO-NO_2-NO_x analyzer and a Thermo Scientific Model 49i ozone analyzer, respectively. Meteorological parameters, including wind speed, wind direction, RH, and temperature were measured by an automatic weather station (MAWS201, Vaisala, Vantaa, Finland) and a wind sensor (Vaisala Model QMW101-M2).

2.3 Data analysis

2.3.1 ACSM data analysis

The standard ACSM data analysis software in Igor Pro (WaveMetrics, Inc., Lake Oswego, Oregon USA) was used to analyze the ACSM dataset. IE was determined by comparing the response factors of ACSM to the mass calculated with the known particle size and the number concentration from a condensation particle counter (CPC, TSI model 3772). Standard relative ionization efficiencies (RIEs) were used for organics, nitrate and chloride (i.e., 1.4 for organics, 1.1 for nitrate and 1.3 for chloride) (Canagaratna et al., 2007) and RIEs for ammonium (6.1) and sulfate (1.2) were estimated from the RIE calibrations using NH_4NO_3 and $(NH_4)_2SO_4$. The collection efficiency (CE) was introduced to correct for the particle loss due to particle bounce, which is influenced by aerosol acidity, composition and the aerosol liquid water content. Considering that the particles were dried before entering the ACSM and are overall neutralized, the influences of aerosol liquid water and acidity are expected to be negligible. Therefore, CE was determined as $CE_{dry} = \max(0.45, 0.0833 + 0.9167 \times ANMF)$, where ANMF represents the mass fraction of ammonium nitrate in NR-PM_1 (Middlebrook et al., 2012).

2.3.2 Source apportionment

PMF was used to perform the source apportionment on the mass spectra of organics as implemented by the multilinear engine (ME-2; Paatero, 1999) via the interface SoFi (Source Finder) coded in Igor Wavemetrics (Canonaco et al., 2013). The OA source apportionment for the summer dataset and the winter dataset was performed separately. First, a range of solutions with different factor numbers from unconstrained runs were examined using conventional PMF. A mixture of two or more factors was found and cannot be separated further for both summer and winter dataset even after increasing the factor number. Then the ME-2 approach was used as it can direct the apportionment towards an environmentally-meaningful solution by introducing *a priori* information (profiles) for certain factors (Canonaco et al., 2013; Crippa et al., 2014; Frohlich et al., 2015). The final results are verified based on the rationality of unconstrained factors, distinct mass spectra, time series and good correlations with external tracers for all factors. Details about the PMF and ME-2 source apportionment are provided in the supplementary information. In this study, four OA factors including hydrocarbon-like OA (HOA), cooking OA (COA), isoprene-oxidized OA (ISOOA) and OOA were resolved during summer, and six OA factors including HOA, COA, biomass burning OA (BBOA), coal combustion OA (CCOA), LO-OOA, and MO-OOA were resolved during winter. Note that MO-OOA and LO-OOA were defined in winter because of much higher $f_{44/43}$ value of MO-OOA (8.6) than that of LO-OOA (2.6) and the large difference in time series of these two factors. Different from the two identified wintertime OOAs, the summertime OOA was mixed and could not be further separated into LO-OOA and MO-OOA, likely due to the limited mass resolution of ACSM (Sun et al., 2012).

2.4 Aerosol liquid water content

Aerosol liquid water content (ALWC) was calculated by the ISORROPIA-II model (Fountoukis and Nenes, 2007) using ACSM aerosol composition and meteorological parameters (temperature and RH) as model inputs. The ISORROPIA-II model then calculated the composition and the phase state of a $NH_4^+–SO_4^{2-}–NO_3^-–Cl^-–H_2O$ system in thermodynamic equilibrium and the concentration of H^+ and ALWC can be resolved.

3. Results and discussion

3.1 Chemical composition of PM_1 in summer and winter

Fig. 1 shows the time series of individual chemical composition of PM_1, OA sources, gaseous species and meteorological parameters in summer and winter. The average values of each components in different periods are summarized in Table 1. As shown in Fig. 1, very different time variations of PM_1 composition, OA sources and gaseous species were observed between summer and winter. The concentrations of gaseous species such as CO, SO_2 and NO_x during winter were ~3 times higher than those during summer, largely due to enhanced emissions and accumulation of pollutants during winter. In contrast, the average O_3 concentration during winter (9.2 ppb) was ~5 times lower than that during summer (49.6 ppb), largely due to titration by enhanced wintertime emissions of NO_x. In summer, meteorological conditions were relatively stable with the wind speeds often being lower than 2 m s^{-1} during the measurement period. The average mass concentration of PM_1 was 41.0 ± 23.4 μg m^{-3} during summer, and OA constituted a major fraction of PM_1 mass (47%), followed by sulfate (18%), ammonium (14%), nitrate (13%), eBC (7%), and chloride (1%). In winter, however, due to frequent changes of meteorological conditions, the time series of PM_1 components and gaseous species varied dramatically, such as the rapid build-up of haze pollution under stagnant meteorological conditions with high RH and low wind speed (< 2 m s^{-1}), or sudden occurrence of clean days because of the dilution by clean air masses from north or northwest at high wind speed (5-10 m s^{-1}). The PM_1 mass concentration with an average value of 63.2 ± 55.1 μg m^{-3} was observed during winter. OA contributed a mass fraction of 49%, followed by nitrate (17%), sulfate (12%), ammonium (12%), eBC (5%), and chloride (5%). As for secondary inorganic species, sulfate is the largest contributor in summer, but replaced by nitrate in winter largely due to different formation processes between summer and winter (as discussed below). An enhancement of chloride from ~1% (0.2 μg m^{-3}) in summer to ~5% (3.1 μg m^{-3}) in winter was also observed, which could be attributed to substantial emissions from coal combustion in winter (Huang et al., 2014; Wang et al., 2015; Elser et al., 2016; Hu et al., 2016).

OA contributed the highest mass fraction to PM_1 in both summer and winter, suggesting the important role of OA in PM_1 pollution (Zhang et al., 2014; Sun et al., 2015; Hu et al., 2016). As for OA sources, the concentration of HOA increased from 1.5 μg m^{-3} during summer to 3.6 μg m^{-3} during winter and the fractional contribution of HOA increased accordingly from 8% to 12%. COA also showed similar increasing trend from summer to winter, with mass concentration increasing from 3.4 μg m^{-3} to 6.3 μg m^{-3} and fractional contribution from 18% to 20%~~, suggesting the enhanced primary emission during winter~~. The increase in mass concentration of COA in winter is likely caused by meteorological conditions (e.g., shallower PBL heights in winter than in summer) because the cooking activities are not expected to have seasonal variation. BBOA and CCOA were only resolved during winter with mass fractions of 9% and 20%, respectively.~~ The BBOA contribution was lower than that observed in wintertime 2010 (Hu et al., 2016), suggesting the efficient control of biomass burning in Beijing and surrounding areas in recent years~~. The average wintertime BBOA concentration decreased from 3.6 μg m^{-3} in 2010 (Hu et al., 2016) to 2.8 μg m^{-3} in 2015 in our study and further to 2.4 μg m^{-3} in 2017-2018 (Li et al., 2019), suggesting efficient control of the biomass burning activities in Beijing and surrounding areas in recent years. Two secondary OA sources (OOA and ISOOA) were resolved during summer. OOA was the dominant OA source during summer due to strong atmospheric oxidation capacity, accounting on average for 69% of total OA with an average mass concentration of 13.0 μg m^{-3}. In addition to OOA, another SOA factor, ISOOA, derived from isoprene-oxidation was resolved in summertime

Beijing. ISOOA was generally thought to be formed in environment with low NOx and high biogenic emissions, but has recently been observed in urban Nanjing in summer 2013 (Zhang et al., 2017). Similar to the result in summertime Nanjing (4% of OA), in our study ISOOA is found to contribute ~5% of total OA with an average mass concentration of 1.0 μg m^{-3} in summertime Beijing. In contrast, ISOOA was not resolved during winter, which is consistent with the low emissions of isoprene. It should be noted that the estimated uncertainty of ISOOA factor is ~20%, suggesting large uncertainty in ISOOA source in urban Beijing. ~~ISOOA contributed ~5% to total OA with an average mass concentration of 1.0 μg m^{-3}, similar to the findings (4%) reported for Nanjing in summer 2013 (Zhang et al., 2017). In contrast, ISOOA was not resolved during winter, which is consistent with the low emissions of isoprene.~~In winter, two OOAs, i.e., LO-OOA and MO-OOA, are identified. The fractional contribution of LO-OOA to total OA (23%, 7.1 μg m^{-3}) was larger than that of MO-OOA (16%, 5.1 μg m^{-3}), suggesting more efficient formation of LO-OOA than MO-OOA during winter. The OOA contribution to total OA decreased from 69% in summer to 39% in winter, mainly due to enhanced primary emission in winter.

We also compared our results with previous studies in Beijing. As shown in Fig. 2, the PM$_1$ mass concentration during summer in our study is similar to that observed during summer 2012 (Hu et al., 2017), but ~30-50% lower than that measured during summer 2008 (Zhang et al., 2013) and summer 2011 (Sun et al., 2015; Hu et al., 2016). From summer 2008 to summer 2015, the fraction contribution of SIA to the PM$_1$ mass decreased from 62% to 45% and the OA contribution increased from 36% to 47%, suggesting the increasing importance of OA ~~in recent years~~ due to the reduction of SO$_2$ and NO$_x$ emissions. Meanwhile, we found that the fractional contribution of SOA (i.e., OOAs herein) to total OA also increased from 60% in summer 2008 to 69% in summer 2015, indicating the increased importance of SOA formation during summer in recent years. From summer 2015 to summer 2018, the PM$_1$ concentration continued decreasing while the SIA contribution was again higher than that during summer 2015 and the SOA faction was similar to that in summer 2015 (Zhou et al., 2019). In winter, the average concentration of PM$_1$ observed in our study was similar to that observed in 2014 (Xu et al., 2018), but lower than most of those in 2008-2013 (Zhang et al., 2013; Zhang et al., 2014; Sun et al., 2013, 2015, 2016; Hu et al., 2016). Especially in winter 2013 enhanced average PM$_1$ concentration of 94.0 μg m^{-3} and 81.7 μg m^{-3} were observed by Zhang et al (2014) and Hu et al (2017), respectively, due to the severe pollution events in January 2013. After 2015, the wintertime PM$_1$ concentration further decreased to 33.2 μg m^{-3} in 2017-2018 (Li et al., 2019), but showed a peak concentration (92.9 μg m^{-3}) in Nov-Dec 2016 because of prevailing air masses from south and northeast of Beijing and high frequencies of high RH and low wind speeds (Xu et al., 2018). Such changes again suggested that the difference in meteorological conditions is one of the major causes of severe particulate pollution in Beijing. The variations of SIA fractions were not obvious from 2008 to 2015 during wintertime with SIA contribution ranged from 34% to 43%, except a higher SIA contribution of 55% observed by Hu et al (2017) in winter 2013. However, from winter 2015 to 2018, the SIA fraction increased from

40% to 54%, suggesting the increased importance of SIA from 2015 to 2018. As for OA, SOA have lower contribution during winter than summer in all years from 2008 to 2018~~5~~. The SOA contributions after 2013 (40%-~~50~~54%) were higher than most of those in 2008-2012 (20%-30%) during wintertime, highlighting the increased importance of SOA in winter.

3.2 Daytime evolution of secondary species in summer and winter

The diurnal cycles of PM$_1$ species and OA sources are shown in Fig. S4. The diurnal variations are affected by the evolution of planetary boundary layer (PBL) height that governs the vertical dispersion of pollutants and by the diurnal cycle of the emissions and atmospheric processes (Huang et al., 2019). To minimize the effects of PBL height and to investigate the daytime processes of secondary species between summer and winter, data of secondary species were normalized by ΔCO because CO is often used as a tracer to account for dilution on timescales of hours to days. As shown in Fig. 3, after offsetting the PBL dilution effect, OOA displayed the fastest increase from 6:00 to 13:00 (local time, LT) with an average growth rate of 2.4 μg m^{-3} ppm^{-1} h^{-1} during summer. Sulfate also showed a clear increasing trend from 6:00 to 17:00 LT with an average growth rate of 1.05 μg m^{-3} ppm^{-1} h^{-1}, indicating the efficient daytime production of OOA and sulfate. However, nitrate displayed a decreasing trend from 11:00 to 18:00 LT, suggesting that evaporation of existing ammonium nitrate was more efficient than production because of its high volatility and thermal instability in the warm afternoon. Associated with sulfate and nitrate, the diurnal cycle of ammonium was affected by both sulfate and nitrate formation mechanisms, which showed a minor increasing trend from 6:00 to 15:00 LT with an average growth rate of 0.48 μg m^{-3} ppm^{-1} h^{-1}. In contrast, all secondary species displayed similar increasing trends from 8:00 to 13:00 LT during winter. Nitrate showed the fastest increasing rate of 1.2 μg m^{-3} ppm^{-1} h^{-1} on average, followed by LO-OOA (1.1 μg m^{-3} ppm^{-1} h^{-1}), ammonium (0.6 μg m^{-3} ppm^{-1} h^{-1}), sulfate (0.48 μg m^{-3} ppm^{-1} h^{-1}) and MO-OOA (0.19 μg m^{-3} ppm^{-1} h^{-1}). The high increasing rate of nitrate in winter compared to summer suggested its enhanced daytime production due to lower temperature. LO-OOA displayed a much clearer increasing trend than that of MO-OOA, suggesting that the daytime formation of LO-OOA was much more efficient than that of MO-OOA during winter, which is consistent with the diurnal cycle of MO-OOA concentration (Fig. S4). It should be noted that although the increase rates of sulfate and SOA (LO-OOA + MO-OOA) during winter were lower than that during summer, the enhancement ratios (about 1.5 times, from 4.0 μg m^{-3} ppm^{-1} to 6.1 μg m^{-3} ppm^{-1} for sulfate; and about 2.0 times, from 5.4 μg m^{-3} ppm^{-1} to 11.4 μg m^{-3} ppm^{-1} for SOA) during winter were similar with that during summer (about 2.0 times, from 10.3 μg m^{-3} ppm^{-1} to 21.9 μg m^{-3} ppm^{-1} for sulfate; and 1.8 times, from 20.7 μg m^{-3} ppm^{-1} to 38.8 μg m^{-3} ppm^{-1} for SOA), indicating that the daytime oxidation formation efficiency of secondary aerosol during winter was comparable to that during summer. Certainly, we note that wintertime photochemistry was traditionally thought to be low because the wintertime OH radical concentrations were traditionally thought to be low due to low O$_3$ concentrations (e.g., 9.2 ppb in winter versus 49.6 ppb in summer in our study) and reduced solar UV level in winter. However, recent measurements of OH radicals at a suburban site of Beijing reported wintertime OH radical concentrations at noontime ranged from 2.4×10^6 cm^{-3} during severe pollution events (k_{OH} ~27 s^{-1}) to 3.6×10^6 cm^{-3} during relatively clean events (k_{OH} ~5 s^{-1}) (Tan et al., 2018). These OH radical concentrations are nearly one order of magnitude larger than those predicted by global models for northern China in winter (Lelieveld et al., 2016). The higher-than-expected OH concentrations and moderate OH reactivity in Beijing resulted in fast photochemistry in winter (Lu et al., 2019), explaining the high contribution of secondary aerosol during wintertime severe haze events (Huang et al., 2014). Meanwhile, there have been increasing evidence showing HONO, instead of O_3, is the main source of OH radicals in wintertime North China Plain (Hendrick et al., 2014; Xing et al., 2019). Further, Lu et al. (2019) found surprisingly high OH radical oxidation rates of up to 15 ppbv h^{-1} in Beijing in winter, which is comparable to that in summer and is mainly initiated by the photolysis of HONO and maintained by an extremely efficient radical cycling process driven by nitric oxide.

3.3 Sulfate and nitrate formation in summer and winter

To elucidate the formation mechanisms of sulfate and nitrate, the correlations between NO_3^- and SO_4^{2-} colored by RH or O_x are shown in Fig. 4. NO_3^- and SO_4^{2-} correlated well in winter with R^2 of 0.6, while there was no good correlation between NO_3^- and SO_4^{2-} in summer. The correlations between NO_3^- and SO_4^{2-} strongly depended on RH and O_x, and this dependence on RH and O_x is reverse between summer and winter. In summer, the correlation between NO_3^- and SO_4^{2-} showed higher slope at higher RH, indicating a faster production ~~growth~~ rate of NO_3^- than SO_4^{2-} in high RH condition. The higher concentration of NO_3^- at high RH was likely due to the transformation of HNO_3 into particle phase, which could be enhanced at high RH and low temperature conditions (Sun et al., 2015). In contrast, the slope of correlation between NO_3^- and SO_4^{2-} decreased as O_x concentration increased, indicating the efficient formation of SO_4^{2-} in high O_x concentration due to photochemical oxidation. On the contrary, in winter both opposite trends related to RH and O_x were observed. Higher NO_3^-/SO_4^{2-} ratio was found at low RH and high O_x conditions and the NO_3^-/SO_4^{2-} ratio decreased dramatically as RH increased due to the fast formation of sulfate in high RH condition. Such variations between summer and winter suggested that in summer photochemical oxidation was perhaps the major pathway of sulfate formation and high RH condition facilitated the nitrate formation due to enhanced gas-to-particle partitioning of NH_4NO_3, while in winter daytime photochemical process played a dominant role in the formation of nitrate and aqueous-phase processes had significant impacts on the formation of sulfate.

This finding is further supported by the effects of RH and O_x on sulfur oxidation ratio (SOR) and nitrogen oxidation ratio (NOR) (Fig. S5). In summer, there was no obvious dependence between SOR and RH, whereas a positive correlation was found between SOR and O_x. NOR was independent of both RH and O_x, the higher nitrate concentration in high RH condition during summer could be attributed to enhanced gas-to-particle partitioning of the highly hydrophilic NH_4NO_3 and the hydrolysis of N_2O_5 (Su et al., 2017). In contrast, SOR shows an evident exponential relationship with RH in winter, indicating the important role of aqueous-phase reaction in the sulfate formation. NOR shows just a small increasing trend with RH, but strongly correlated with O_x concentration, suggesting the major role of photochemical oxidation in the nitrate formation during winter. It should be noted that SOR also displayed an increasing trend as O_x increased during winter, implying the role of photochemical process in the sulfate formation and high RH condition still promoted the gas-to-particle partitioning of nitrate. However, as the aqueous-phase reaction leads enhanced sulfate formation during winter, the ratio of NO_3^-/SO_4^{2-} decreased as RH increased.

It is noted that the diurnal variations of $SO_4^{2-}/\triangle CO$ and $NO_3^-/\triangle CO$ were similar in winter (Fig. 3). However, the increasing rate of $SO_4^{2-}/\triangle CO$ was much lower than that of $NO_3^-/\triangle CO$. Also the absolute concentration of wintertime sulfate showed a decreasing trend in the afternoon, consistent with the diurnal variations of RH and ALWC, while the absolute concentration of wintertime nitrate showed an increasing trend from 8:00 to 18:00 LT (Fig. S4). These results further suggest the difference in dominant formation processes between sulfate and nitrate in winter. The photochemical processes were likely the dominant pathways for daytime nitrate formation but less important for sulfate formation because of large contributions from aqueous-phase processes as indicated by the exponential relationship between SOR and RH in wintertime Beijing (Fig. S5d).

3.4 SOA formation in summer and winter

The relationships between OOA and O_x or ALWC during summer are shown in Fig. 5. It should be note that a majority of the data are scattering, therefore caution should be given for the uncertainties when using O_x and ALWC as indicators of photochemical processing and aqueous processing, respectively. The mass fraction of OOA to OA (f_{OOA}) is positively correlated with O_x, increasing from 0.61 to 0.75 when O_x concentration increases from 20 ppb to 150 ppb, suggesting that photochemical oxidation may play a key role in the OOA formation during summer in Beijing. In contrast, f_{OOA} was independent of ALWC during summer. Consistently, the mass concentration of OOA was also positively correlated with O_x concentration, whereas higher RH was usually located at the left-bottom corner with low O_x concentration and low OOA concentration (Fig. 5c). This suggests that RH has ~~either no effects or~~ relatively minor but complex effects on the formation of OOA during summer~~formation~~. During winter, although the f_{OOA} (mass fraction of LO-OOA + MO-OOA to total OA) showed no clear increase or decrease trends with O_x or ALWC (Fig.5 e, f), the correlation between the mass concentration of OOA (total mass of LO-OOA+MO-OOA) and O_x becomes stronger compared with that during summer. Higher OOA concentration was usually related to both higher O_x concentration and higher RH (Fig. 5g). Meanwhile, the increase trend of OOA concentration with ALWC was also more clear in winter than in summer.

These suggest that both photochemical oxidation and aqueous-phase reaction play roles in the OOA formation during winter in Beijing. It should be noted that temperature could affect both atmospheric oxidative capacity and RH and therefore the photochemistry and aqueous-phase processes. As shown in Fig. S6, both mass concentration and mass fraction of OOA showed positive correlations with temperature, suggesting that high temarature promotes the oxidation and formation of OOA in summer. Further analysis shows a positive corralation between temparature and Ox ($R^2 = 0.59$) and a strong negative correlation between temperature and RH ($R^2 = 0.63$). This indicates that high temperature conditions in summer corresponded to high Ox and low RH conditions, further confirming the relatively important role of photochemical oxidation than aqueous-phase processes in the OOA formation during summer. In winter, however, both mass concentration and mass fraction of OOA (or LO-OOA and MO-OOA) showed no clear correlation with temperature. Also, there was no clear correlation between temperature and Ox or RH, suggesting a more complex effects of temperature on the SOA formation in winter.

The difference in daytime increasing rate of LO-OOA and MO-OOA suggests potential difference in their formation during winter (Fig. 3b). The correlations of the two identified OOAs with O_x and ALWC are investigated in Fig. 6. A clear positive correlation between the mass concentration of LO-OOA and O_x is shown ($R^2 = 0.51$ for the entire data), while the correlation between LO-OOA and ALWC is weaker. Consistently, the correlation coefficient between the mass concentration of LO-OOA and O_x decreased from 0.61 at RH < 60% to 0.29 at RH > 60% (Fig. 6a). The fractional contribution of LO-OOA to total OA increased from 0.17 to 0.35 as O_x concentration increased from 30 ppb to 60 ppb when RH < 60%, mainly driven by the increased LO-OOA concentrations as O_x increases. The fractional contribution of LO-OOA however decreased from 0.25 to 0.18 when ALWC increased from 15 μg m^{-3} to 300 μg m^{-3} (Fig. 6d), explained by the more efficient formation of MO-OOA at high RH conditions during winter. Consistently, the mass concentration of MO-OOA showed a strong positive correlation with ALWC during winter with R^2 of 0.6, while the correlations between MO-OOA and O_x are weaker than those of LO-OOA both at RH < 60% and RH > 60%. The fractional contribution of MO-OOA increased clearly from 0.14 to 0.25 when ALWC increased from 60 μg m^{-3} to 350 μg m^{-3}, but decreased from 0.3 to 0.18 when O_x concentration increased from 30 ppb to 70 ppb. Similarly, there was a good correlaiton between the ratio of LO-OOA/MO-OOA and O_x concentration when RH < 60% and there was no significant dependence of LO-OOA/MO-OOA on O_x concentration when RH > 60% (Fig. 7). Our results indicate that O_x likely played a more important role in the LO-OOA formation whereas ALWC was more important for the MO-OOA formation in winter. The dependence of LO-OOA as well as the mass ratio of LO-OOA to MO-OOA on atmospheric oxidative tracer (i.e., O_x) both degraded when RH were greater than 60%, suggesting that RH or aerosol liquid water may also affect the LO-OOA formation.

3.5 Evolution from clean days to pollution days

In order to better understand the aerosol evolution from clean days to pollution days between summer and winter, PM_1 composition and OA sources in clean days (daily average PM_1 < 20 μg m^{-3}) and pollution days (daily average PM_1 > 40 μg m^{-3} in summer and daily average PM_1 > 60 μg m^{-3} in winter) were analyzed. As shown in Fig. 8, the PM_1 composition shows similar evolution trends from clean days to pollution days in both seasons, with increase of SIA contribution and decrease of OA contribution, suggesting the enhanced formation of SIA during pollution period. Specifically, the PM_1 mass increased from 13.7 μg m^{-3} during clean days to 59.2 μg m^{-3} during pollution days in summer, with OA fraction decreasing from 60% to 44% and SIA fraction increasing from 29% to 48%. In comparison, during winter the average mass concentration of PM_1 was 115.5 μg m^{-3} during polluted days, which was ten times higher than that during clean days (10.2 μg m^{-3}). The mass fraction of OA decreased from 55% during clean days to 48% during pollution days and SIA fraction increased from 36% to 41% accordingly. As for OA, the mass concentrations increased substantially during both summer and winter. In summer, the mass fraction of SOA increased from 70% in clean days to 76% in pollution days along with 3 times greater mass of OA, indicating the importance of SOA formation during pollution events in summer. It should be noted that ISOOA had similar contributions to OA between clean days (5%) and pollution days (5%) with the mass concentration increasing from 0.4 μg m^{-3} to 1.3 μg m^{-3} and the increase in SOA contribution was mainly from OOA. In winter, although the mass fraction of SOA (LO-OOA and MO-OOA) decreased from 44% during clean days to 39% during pollution days, their mass concentrations increased by 8 times. The mass fraction of POA (HOA, COA, BBOA and CCOA) increased from 56% to 61%, indicating that primary contributions are as important as secondary contributions for OA during pollution in winter.

To further investigate the effect of RH on aerosol composition, we separated the pollution days to high-RH pollution days (H-RH, RH > 60%) and low-RH pollution days (L-RH, RH < 40%) in summer and winter. As shown in Fig. 8, the PM_1 concentration during L-RH pollution days (60.7 μg m^{-3}) was similar to that during H-RH pollution days (58.3 μg m^{-3}) during summer. Interestingly, the mass concentration of sulfate decreased dramatically from 18.3 μg m^{-3} during L-RH pollution days to 9.2 μg m^{-3} during H-RH pollution days and the mass fraction decreased accordingly from 30% to 16% in summer. The concentration of nitrate increased from 5.1 μg m^{-3} during L-RH pollution days to 10.9 μg m^{-3} during H-RH pollution days and the mass fraction increased accordingly from 8% to 19%. In contrast, during winter the PM_1 concentration during H-RH pollution days (121.4 μg m^{-3}) was higher than that during L-RH pollution days (89.5 μg m^{-3}). The mass fraction of sulfate increased from 6% during L-RH pollution days to 14% during H-RH pollution days and the mass concentration increased accordingly from 5.8 μg m^{-3} to 16.8 μg m^{-3}, while the mass fraction of nitrate decreased from 21% during L-RH pollution days to 16% during H-RH pollution days with similar mass concentration of 18.6 μg m^{-3} and 19.0 μg m^{-3} respectively. The difference of sulfate and nitrate behavior for L-RH and H-RH polluted days in summer and winter suggests that there are factors controlling their production related to aqueous-phase processing other than RH or aerosol liquid water content (e.g., precursors, catalyst, and temperature).

As for SOA, the concentration of OOA decreased from 18.4 μg m^{-3} during L-RH pollution days to 17.0 μg m^{-3} during H-RH pollution days with the mass fraction decreasing from 75% to 68%. Note that the low RH condition is often related to high temperature and strong oxidation capacity, which facilitates photochemical production during summer. As is consistent with previous understanding of different importance of photochemical and aqueous production for the two OOAs, the LO-OOA and MO-OOA in winter vary differently between L-RH pollution days and H-RH pollution days. The mass fraction of MO-OOA increased from 12% during L-RH pollution days to 17% during H-RH pollution days and the mass concentration increased accordingly from 5.8 μg m^{-3} to 9.9 μg m^{-3}. On the contrary, the mass fraction of LO-OOA decreased from 34% during L-RH pollution days to 20% during H-RH pollution days with mass concentration decreasing from 16.1 μg m^{-3} to 11.7 μg m^{-3}.

4. Conclusion

In this study, variations of PM_1 composition, OA sources and secondary formation processes between summer and winter in urban Beijing were analyzed. PM_1 composition revealed the increase of SIA contribution and decrease of OA contribution during polluted days when compared to clean days, suggesting the important role of SIA during haze pollution. Higher mass ratio of sulfate to nitrate during L-RH pollution in summer whereas during H-RH pollution in winter were observed. The analysis of RH and O_x effects indicated that photochemical oxidation was probably the major pathway of sulfate production during summer while the importance of aqueous-phase reaction increased during winter. In contrast, much higher nitrate (17%) was found during winter due to preferable gas-to-particle partitioning at low temperature, while higher nitrate (19%) was also observed under the condition of high relative humidity during summer likely due to enhanced gas-to-particle partitioning of hydrophilic NH_4NO_3 and the hydrolysis of N_2O_5. As for OA sources, SOA dominated OA mass (74%) during summer while the SOA contribution decreased to 39% during winter due to enhanced primary emission in heating season. OOA had higher concentration and fraction during L-RH pollution days than during H-RH pollution days in summer, indicating the possibility of control factors other than RH or aerosol liquid water for aqueous processing. Summertime OOA was likely dominated by gas-phase photochemical process given the good correlation between OOA and O_x. In comparison, MO-OOA increased during H-RH pollution days in winter while the LO-OOA decreased during H-RH pollution days, indicating that the formation of MO-OOA was perhaps promoted by the aqueous-phase processes, while gas-phase photochemical oxidation facilitates the LO-OOA formation during winter. These conclusions were supported by the good correlation between LO-OOA and O_x as well as tight correlation between MO-OOA and ALWC during winter. Meanwhile, we found that the dependence of LO-OOA as well as the mass ratio of LO-OOA to MO-OOA on O_x both degraded under conditions of RH > 60%, suggesting that RH or aerosol liquid water may also affect the LO-OOA formation.

Data availability. Raw data used in this study are archived at the Institute of Earth Environment, Chinese Academy of Sciences, and are available on request by contacting the corresponding author.

Supplement. The Supplement related to this article is available online at

Author contributions. RJH designed the study. Data analysis and source apportionment were done by JD, RJH and QC. JD and RJH wrote the manuscript. JD and RJH interpreted data and prepared display items. All authors commented on and discussed the manuscript.

Competing interests. Douglas R. Worsnop is an employee of Aerodyne Research, Inc. (ARI), and an ACSM produced by Aerodyne was used in this study.

Acknowledgements. This work was supported by the National Natural Science Foundation of China (NSFC) under grant no. 91644219, no. 41877408 and no. 21661132005, the Chinese Academy of Sciences (no. ZDBS-LY-DQC001), and the National Key Research and Development Program of China (no. 2017YFC0212701). The authors acknowledge financial support from the Cross Innovative Team fund from the State Key Laboratory of Loess and Quaternary Geology (SKLLQG) (no. SKLLQGTD1801). The authors also thank Weikang Ran for assistance in field measurements.

Reference

An, Z., Huang, R.-J., Zhang, R., Tie, X., Li, G., Cao, J., Zhou, W., Shi, Z., Han, Y., Gu, Z., and Ji, Y.: Severe haze in northern China: A synergy of anthropogenic emissions and atmospheric processes, Proc. Natl. Acad. Sci., 116(18), 8657–8666, https://doi.org/10.1073/pnas. 1900125116, 2019.

Canagaratna, M. R., Jayne, J. T., Jimenez, J. L., Allan, J. D., Alfarra, M. R., Zhang, Q., Onasch, T. B., Drewnick, F., Coe, H., Middlebrook, A., Delia, A., Williams, L. R., Trimborn, A. M., Northway, M. J., DeCarlo, P. F., Kolb, C. E., Davidovits, P., and Worsnop, D. R.: Chemical and microphysical characterization of ambient aerosols with the Aerodyne aerosol mass spectrometer, Mass Spectro. Rev., 26(2), 185–222, https://doi.org/10.100/mas. 20115, 2007.

Canonaco, F., Crippa, M., Slowik, J. G., Baltensperger, U., and Prévôt, A. S. H.: SoFi, an IGOR-based interface for the efficient use of the generalized multilinear engine (ME-2) for the source apportionment: ME-2 application to aerosol mass spectrometer data, Atmos. Meas. Tech., 6, 3649–3661, https://doi.org/10.5194/amt-6-3649-2013, 2013.

Cheng, Y. F., Zheng, G. J., Wei, C., Mu, Q., Zheng, B., Wang, Z. B., Gao, M., Zhang, Q., He, K. B., Carmichael, G., Pöschl, U., and Su, H.: Reactive nitrogen chemistry in aerosol water as a source of sulfate during haze events in China, Science Advances, 2(12), e1601530, https://doi.org/10.1126/sciadv.1601530, 2016.

Crippa, M., Canonaco, F., Lanz, V. A., Äijälä, M., Allan, J. D., Carbone, S., Capes, G., Ceburnis, D., Dall'Osto, M., Day, D. A., DeCarlo, P. F., Ehn, M., Eriksson, A., Freney, E., Hildebrandt Ruiz, L., Hillamo, R., Jimenez, J. L., Junninen, H., Kiendler-Scharr, A., Kortelainen, A. M., Kulmala, M., Laaksonen, A., Mensah, A. A., Mohr, C., Nemitz, E., O'Dowd, C., Ovadnevaite, J., Pandis, S. N., Petäjä, T., Poulain, L., Saarikoski, S., Sellegri, K., Swietlicki, E., Tiitta, P., Worsnop, D. R., Baltensperger, U., and Prévôt, A. S. H.: Organic aerosol components derived from 25 AMS data sets across Europe using a consistent ME-2 based source apportionment approach, Atmos. Chem. Phys., 14, 6159–6176, https://doi.org/10. 5194/acp-14-6159-2014, 2014.

Ding, A. J., Huang, X., Nie, W., Sun, J. N., Kerminen, V. M., Petäjä, T., Su, H., Cheng, Y. F., Yang, X. Q., Wang, M. H., Chi, X. G., Wang, J. P., Virkkula, A., Guo, W. D., Yuan, J., Wang, S. Y., Zhang, R. J., Wu, Y. F., Song, Y., Zhu, T., Zilitinkevich, S., Kulmala, M., and Fu, C. B.: Enhanced haze pollution by black carbon in megacities in China, Geophys. Res. Lett., 43, 2873–2879, https://doi.org/10.1002/2016GL067745, 2016.

Duan, J., Huang, R.-J., Lin, C., Dai, W., Wang, M., Gu, Y., Wang, Y., Zhong, H., Zheng, Y., Ni, H., Dusek, U., Chen, Y., Li, Y., Chen, Q., Worsnop, D. R., O'Dowd, C. D., and Cao, J.: Distinctions in source regions and formation mechanisms of secondary aerosol in Beijing from summer to winter, Atmos. Chem. Phys., 19, 10319–10334, https://doi.org/10.5194/acp-19-10319-2019, 2019.

Elser, M., Huang, R. J., Wolf, R., Slowik, J. G., Wang, Q., Canonaco, F., Li, G., Bozzetti, C., Daellenbach, K. R., Huang, Y., Zhang, R., Li, Z., Cao, J., Baltensperger, U., El-Haddad, I., and Prévôt, A. S. H.: New insights into PM2.5 chemical composition and sources in two major cities in China during extreme haze events using aerosol mass spectrometry, Atmos. Chem. Phys., 16, 3207–3225, https://doi.org/10.5194/acp-16-3207-2016, 2016.

Fontes, T., Li, P. L., Barros, N., and Zhao, P. J.: Trends of PM2.5 concentrations in China: A long term approach, J. Environ. Manage. 196, 719–732, https://doi.org/10.1016/j.jenvman.2017.03.074, 2017.

Fountoukis, C., and Nenes, A.: ISORROPIA II: a computationally efficient thermodynamic equilibrium model for K^+–Ca^{2+}–Mg^{2+}–NH_4^+–Na^+–SO_4^{2-}–NO_3^-–Cl^-–H_2O aerosols, Atmos. Chem. Phys., 7, 4639–4659, 2007.

Fröhlich, R., Crenn, V., Setyan, A., Belis, C. A., Canonaco, F., Favez, O., Riffault, V., Slowik, J. G., Aas, W., Aijälä, M., Alastuey, A., Artiñano, B., Bonnaire, N., Bozzetti, C., Bressi, M., Carbone, C., Coz, E., Croteau, P. L., Cubison, M. J., Esser-Gietl, J. K., Green, D. C., Gros, V., Heikkinen, L., Herrmann, H., Jayne, J. T., Lunder, C. R., Minguillón, M. C., Mocnik, G., O'Dowd, C. D., Ovadnevaite, J., Petralia, E., Poulain, L., Priestman, M., Ripoll, A., Sarda-Estève, R., Wiedensohler, A., Baltensperger, U., Sciare, J., and Prévôt, A. S. H.: ACTRIS ACSM intercomparison-Part 2: intercomparison of ME-2 organic source apportionment results from 15 individual, co-located aerosol mass spectrometers, Atmos. Meas. Tech., 8, 2555–2576, https://doi.org/10.5194/amt-8-2555-

2015, 2015.

Guo, H., Weber, R. J., Nenes, A.: High levels of ammonia do not raise fine particle pH sufficiently to yield nitrogen oxide-dominated sulfate production, Sci. Rep., 7(1), 12109, 2017.

Hendrick, F., Müller, J. F., Clémer, K., Wang, P., De Mazière, M., Fayt, C., Gielen, C., Hermans, C., Ma, J. Z., Pinardi, G., Stavrakou, T., Vlemmix, T., and Van Roozendael, M.: Four years of ground-based MAX-DOAS observations of HONO and NO2 in the Beijing area, Atmos. Chem. Phys., 14, 765–781, 2014.

Hu, W., Hu, M., Hu, W., Jimenez, J. L., Yuan, B., Chen, W., Wang, M., Wu, Y., Chen, C., Wang, Z., Peng, J., Zeng, L., and Shao, M.: Chemical composition, sources, and aging process of submicron aerosols in Beijing: Contrast between summer and winter, J. Geophys. Res. Atmos., 121(4), 1955–1977, https://doi.org/10.1002/2015JD024020, 2016.

Hu, W., Hu, M., Hu, W.-W., Zheng, J., Chen, C., Wu, Y., and Guo, S.: Seasonal variations in high time-resolved chemical compositions, sources, and evolution of atmospheric submicron aerosols in the megacity Beijing, Atmos. Chem. Phys., 17, 9979–10000, https://doi.org/10.5194/acp-17-9979-2017, 2017.

Huang, R. J., Zhang, Y. L., Bozzetti, C., Ho, K. F., Cao, J. J., Han, Y. M., Daellenbach, K. R., Slowik, J. G., Platt, S. M., Canonaco, F., Zotter, P., Wolf, R., Pieber, S. M., Bruns, E. A., Crippa, M., Ciarelli, G., Piazzalunga, A., Schwikowski, M., Abbaszade, G., Schnelle-Kreis, J., Zimmermann, R., An, Z., Szidat, S., Baltensperger, U., Haddad, I.E., and Prevot, A.S.H.: High secondary aerosol contribution to particulate pollution during haze events in China, Nature, 514, 218–222, 2014.

Huang, R.-J., Wang, Y., Cao, J., Lin, C., Duan, J., Chen, Q., Li, Y., Gu, Y., Yan, J., Xu, W., Fröhlich, R., Canonaco, F., Bozzetti, C., Ovadnevaite, J., Ceburnis, D., Canagaratna, M. R., Jayne, J., Worsnop, D. R., El-Haddad, I., Prévôt, A. S. H., and O'Dowd, C. D.: Primary emissions versus secondary formation of fine particulate matter in the most polluted city (Shijiazhuang) in North China, Atmos. Chem. Phys., 19, 2283–2298, https://doi.org/10.5194/acp-19-2283-2019, 2019.

Lelieveld, J., Gromov, S., Pozzer, A., and Taraborrelli, D.: Global tropospheric hydroxyl distribution, budget and reactivity, Atmos. Chem. Phys., 16, 12477–12493, https://doi.org/10.5194/acp-16-12477-2016, 2016.

Li, G., Bei, N., Cao, J., Huang, R., Wu, J., Feng, T., Wang, Y., Liu, S., Zhang, Q., Tie, X., Molina, L. T.: A possible pathway for rapid growth of sulfate during haze days in China, Atmos. Chem. Phys., 17, 3301–3316, https://doi.org/10.5194/acp-17-3301-2017, 2017.

Li, H., Cheng, J., Zhang, Q., Zheng, B., Zhang, Y., Zheng, G., and He, K.: Rapid transition in winter aerosol composition in Beijing from 2014 to 2017: response to clean air actions, Atmos. Chem. Phys., 19, 11485–11499, https://doi.org/10.5194/acp-19-11485-2019, 2019.

Liu, M., Song, Y., Zhou, T., Xu, Z., Yan, C., Zheng, M., Wu, Z., Hu, M., Wu, Y., and Zhu, T.: Fine particle pH during severe haze episodes in northern China, Geophys. Res. Lett., 44(10), 5213-5221, 2017.

Lu, K., Fuchs, H., Hofzumahaus, A., Tan, Z., Wang, H., Zhang, L., Schmitt, S., Rohrer, F., Bohn, B., Broch, S., Dong, H., Gkatzelis, G., Hohaus, T., Holland, F., Li, X., Liu, Y., Liu, Y. H., Ma, X., Novell, A., Schlag, P., Shao, M., Wu, Y., Wu, Z., Zeng, L., Hu, M., Kiendler-Scharr, A., Wahner, A., and Zhang, Y.: Fast Photochemistry in Wintertime Haze: Consequences for Pollution Mitigation Strategies, Environ. Sci. Technol., 53(18), 10676-10684, 2019.

Middlebrook, A. M., Bahreini, R., Jimenez, J. L., and Canagaratna, M. R.: Evaluation of composition-dependent collection efficiencies for the Aerodyne aerosol mass spectrometer using field data, Aerosol Sci. Tech., 46 (3), 258–271, https://doi.org/10.1080/02786826.2011.620041, 2012.

Ng, N. L., Herndon, S. C., Trimborn, A., Canagaratna, M. R., Croteau, P. L., Onasch, T. B., Sueoer, D., Worsnop, D. R., Zhang, Q., Sun, Y. L., and Jayne, J. T.: An Aerosol Chemical Speciation Monitor (ACSM) for routine monitoring of the composition and mass concentrations of ambient aerosol, Aerosol Sci. Technol., 45 (7), 770–784, https://doi.org/10.1080/02786826.2011.560211, 2011.

Paatero, P.: The multilinear engine: a table-driven, least squares program for solving multilinear problems, including the n-way parallel factor analysis model, J. Comput. Graph. Stat., 8, 854–888, https://doi.org/10.1080/10618600.1999.10474853, 1999.

Petäjä, T., Järvi, L., Kerminen, V. M., Ding, A. J., Sun, J. N., Nie, W., Kujansuu, J., Virkkula, A., Yang, X., Fu, C. B., Zilitinkevich, S., and Kulmala, M.: Enhanced air pollution via aerosol-boundary layer feedback in China, Sci. Rep., 6, 18998, 2016.

Su, X., Tie, X. X., Li, G. H., Cao, J. J., Huang, R. J., Feng, T., Long, X., and Xu, R. G.: Effect of hydrolysis of N_2O_5 on nitrate and ammonium formation in Beijing China: WRF-Chem model simulation, Sci. Total. Environ., 579, 221-229, https://doi.org/10.1016/j.scitotenv.2016.11.125, 2017.

Sun, Y. L., Wang, Z., Dong, H., Yang, T., Li, J., Pan, X., Chen, P., and Jayne, J. T.: Characterization of summer organic and inorganic aerosols in Beijing, China with an Aerosol Chemical Speciation Monitor, Atmos. Environ., 51, 250–259, https://doi.org/10.1016/j.atmosenv.2012.01.013, 2012.

Sun, Y. L., Wang, Z. F., Fu, P. Q., Yang, T., Jiang, Q., Dong, H. B., Li, J., and Jia, J. J.: Aerosol composition, sources and processes during wintertime in Beijing, China, Atmos. Chem. Phys., 13, 4577–4592, https://doi.org/10.5194/acp-13-4577-2013, 2013.

Sun, Y., Jiang, Q., Wang, Z., Fu, P., Li, J., Yang, T., and Yin, Y.: Investigation of the sources and evolution processes of severe haze pollution in Beijing in January 2013, J. Geophys. Res. Atmos., 119, 4380–4398, https://doi.org/10.1002/2014JD021641, 2014.

Sun, Y. L., Wang, Z. F., Du, W., Zhang, Q., Wang, Q. Q., Fu, P. Q., Pan, X., Li, J., Jayne, J., and Worsnop, D. R.: Long-term real-time measurements of aerosol particle composition in Beijing, China: seasonal variations, meteorological effects, and source analysis, Atmos. Chem. Phys., 15, 10149–10165, https://doi.org/10.5194/acp-15-10149-2015, 2015.

Sun, Y., Du, W., Fu, P., Wang, Q., Li, J., Ge, X., Zhang, Q., Zhu, C., Ren, L., Xu, W., Zhao, J., Han, T., Worsnop, D. R., and Wang, Z.: Primary and secondary aerosols in Beijing in winter: sources, variations and processes, Atmos. Chem. Phys., 16, 8309–8329, https://doi.org/10.5194/acp-16-8309-

2016, 2016.

Sun, Y., Xu, W., Zhang, Q., Jiang, Q., Canonaco, F., Prévôt, A. S., Fu, P., Li, J., Jayne, J., Worsnop, D. R., and Wang, Z.: Source apportionment of organic aerosol from two-year highly time-resolved measurements by an aerosol chemical speciation monitor in Beijing, China, Atmos. Chem. Phys., 18(12), 8469–8489, 2018.

Takegawa, N., Miyakawa, T., Kuwata, M., Kondo, Y., Zhao, Y., Han, S., Kita, K., Miyazaki, Y., Deng, Z., Xiao, R., Hu, M., van Pinxteren, D., Herrmann, H., Hofzumahaus, A., Holland, F., Wahner, A., Blake, D.R., Sugimoto, N., and Zhu, T.: Variability of submicron aerosol observed at a rural site in Beijing in the summer of 2006, J. Geophys. Res., 114, D00G05, https://doi.org/10.1029/2008jd010857, 2009.

Tan, Z., Rohrer, F., Lu, K., Ma, X., Bohn, B., Broch, S., Dong, H., Fuchs, H., Gkatzelis, G. I., Hofzumahaus, A., Holland, F., Li, X., Liu, Y., Liu, Y., Novelli, A., Shao, M., Wang, H., Wu, Y., Zeng, L., Hu, M., Kiendler-Scharr, A., Wahner, A., and Zhang, Y.: Wintertime photochemistry in Beijing: observations of ROx radical concentrations in the North China Plain during the BEST-ONE campaign, Atmos. Chem. Phys., 18, 12391–12411, https://doi.org/10.5194/acp-18-12391-2018, 2018.

Tie, X., Huang, R. J., Cao, J., Zhang, Q., Cheng, Y., Su, H., Chang, D., Pöschl, U., Hoffmann, T., Dusek, U., Li, G. H., Worsnop, D. R., and O'Dowd, C. D.: Severe pollution in China amplified by atmospheric moisture, Sci. Rep., 7(1),15760, 2017.

Wang, G. H., Zhang, R. Y., Gomez, M. E., Yang, L. X., Zamora, M. L., Hu, M., Lin, Y., Peng, J. F., Guo, S., Meng, J. J., Li, J. J., Cheng, C. L., Hu, T. F., Ren, Y. Q., Wang, Y. S., Gao, J., Cao, J. J., An, Z. S., Zhou, W. J., Li, G. H., Wang, J. Y., Tian, P. F., Marrero-Ortiz, W., Secrest, J., Du, Z. F., Zheng, J., Shang, D. J., Zeng, L. M., Shao, M., Wang, W. G., Huang, Y., Wang, Y., Zhu, Y. J., Li, Y. X., Hu, J. X., Pan, B., Cai, L., Cheng, Y. T., Ji, Y. M., Zhang, F., Rosenfeld, D., Liss, P. S., Duce, R. A., Kolb, C. E., and Molina, M. J.: Persistent sulfate formation from London Fog to Chinese haze, Proc. Natl. Acad. Sci. U.S.A., 113(48), 13630–13635, 2016.

Wang, Q., Sun, Y., Jiang, Q., Du, W., Sun, C., Fu, P., and Wang, Z.: Chemical composition of aerosol particles and light extinction apportionment before and during the heating season in Beijing, China, J. Geophys. Res. Atmos., 120(24), 12708–12722, https://doi.org/10.1002/2015JD023871, 2015.

Wang, Y. C., Huang, R. J., Ni, H. Y., Chen, Y., Wang, Q. Y., Li, G. H., Tie, X. X., Shen, Z. X., Huang, Y., Liu, S. X., Dong, W. M., Xue, P., Fröhlich, R., Canonaco, F., Elser, M., Daellenbach, K.R., Bozzetti, C., Haddad, EI., and Cao, J. J.: Chemical composition, sources and secondary processes of aerosols in Baoji city of northwest China, Atmos. Environ., 158, 128–137, https://doi.org/10.1016/j.atmosenv.2017.03.026, 2017.

Xing, L., Wu, J., Elser, M., Tong, S., Liu, S., Li, X., Liu, L., Cao, J., Zhou, J., El-Haddad, I., Huang, R., Ge, M., Tie, X., Prévôt, A. S. H., and Li, G.: Wintertime secondary organic aerosol formation in Beijing–Tianjin–Hebei (BTH): contributions of HONO sources and heterogeneous reactions, Atmos. Chem. Phys., 19, 2343–2359, https://doi.org/10.5194/acp-19-2343-2019, 2019.

Xu, W. Q., Han, T. T., Du, W., Wang, Q. Q., Chen, C., Zhao, J., Zhang, Y. J., Li, J., Fu, P. Q., Wang, Z. F., Worsnop, D. R., and Sun, Y. L.: Effects of Aqueous-Phase and Photochemical Processing on Secondary Organic Aerosol Formation and Evolution in Beijing, China, Environ. Sci. Technol., 51(2), 762–770, https://doi.org/10.1021/acs.est.6b04498, 2017.

Xu, W. Q., Sun, Y. L., Wang, Q. Q., Zhao, J., Wang, J. F., Ge, X. L., Xie, C. H., Zhou, W., Du, W., Li, J., Fu, P. Q., Wang, Z. F., Worsnop, D. R., and Coe, H.: Changes in aerosol chemistry from 2014 to 2016 in winter in Beijing: insights from high resolution aerosol mass spectrometry, J. Geophys. Res. Atmos., 124(2), 1132–1147, 2018.

Yang, Y. R., Liu, X. G., Qu, Y., An, J. L., Jiang, R., Zhang, Y. H., Sun, Y. L., Wu, Z. J., Zhang, F., Xu, W. Q., and Ma, Q. X.: Characteristics and formation mechanism of continuous hazes in China: a case study during the autumn of 2014 in the North China Plain, Atmos. Chem. Phys., 15, 8165–8178, https://doi.org/10.5194/acp-15-8165-2015, 2015.

Zhang, J. K., Sun, Y., Liu, Z. R., Ji, D. S., Hu, B., Liu, Q., and Wang, Y. S.: Characterization of submicron aerosols during a month of serious pollution in Beijing, 2013, Atmos. Chem. Phys., 14, 2887-2903, https://doi.org/10.5194/acp-14-2887-2014, 2014.

Zhang, Y., Sun, J., Zhang, X., Shen, X., Wang, T., and Qin, M.: Seasonal characterization of components and size distributions for submicron aerosols in Beijing, Sci. China Earth Sci., 56, 890–900, https://doi.org/10.1007/s11430-012-4515-z, 2013.

Zhang, Y. J., Tang, L. L., Sun, Y. L., Favez, O., Canonaco, F., Albinet, A., Couvidat, F., Liu, D. T., Jayne, J. T., Wang, Z., Croteau, P. L., Canagaratna, M. R., Zhou, H. C., Prevot, A. S. H., and Worsnop, D.R.: Limited formation of isoprene epoxydiols-derived secondary organic aerosol under NOx-rich environments in Eastern China, Geophys. Res. Lett., 44(4), 2035–2043, https://doi.org/10.1002/2016GL072368, 2017.

Zhou, W., Gao, M., He, Y., Wang, Q., Xie, C., Xu, W., Zhao, J., Du, W., Qiu, Y., Lei, L., Fu, P., Wang, Z., Worsnop, D.R., Zhang, Q., and Sun, Y.: Response of aerosol chemistry to clean air action in Beijing, China: Insights from two-year ACSM measurements and model simulations, Environ. Pollut., 255, 113345, 2019.

Table 1. Summary of mass concentrations of aerosol species, gaseous pollutants and meteorological parameters during different periods between summer and winter in Beijing.

Species	Summer				Winter			
	Entire Study	Clean	L-RH Pollution	H-RH Pollution	Entire Study	Clean	L-RH Pollution	H-RH Pollution
Aerosol species (μg m^{-3})								
PM$_1$	41.0	13.7	60.7	58.3	63.2	10.2	89.5	121.4
OA	19.1	8.3	24.6	25.1	31.2	5.6	47.8	57.8
HOA	1.5	0.8	1.6	1.7	3.6	0.4	2.9	8.9
COA	3.4	1.7	3.1	4.7	6.3	1.4	11.3	9.6
CCOA	-	-	-	-	6.1	1.0	9.1	11.6
BBOA	-	-	-	-	2.8	0.3	2.6	6.0
ISOOA	1.0	0.4	1.2	1.3	-	-	-	-
OOA	13.0	5.4	18.4	17.0	-	-	-	-
LO-OOA	-	-	-	-	7.1	1.0	16.1	11.7
MO-OOA	-	-	-	-	5.1	1.4	5.8	9.9
SO_4^{2-}	7.5	1.7	18.3	9.2	7.6	1.4	5.8	16.8
NO_3^-	5.6	0.9	5.1	10.9	10.5	1.2	18.6	19.0
NH_4^+	5.7	1.4	10.1	8.5	7.4	1.1	9.8	14.6
Cl^-	0.2	0.1	0.2	0.3	3.1	0.3	3.9	6.2
eBC	2.9	1.3	2.4	4.3	3.4	0.6	3.6	7.0
Gaseous pollutants								
SO_2 (ppb)	3.8	3.0	6.5	3.8	10.8	4.5	14.2	16.1
CO (ppm)	0.6	0.4	0.7	0.6	1.8	0.5	1.7	3.7
NO (ppb)	4.8	4.8	6.8	4.5	34.9	5.4	24.9	79.3
NO_2 (ppb)	21.5	19.4	11.7	23.4	33.2	14.9	43.7	50.3
O_3 (ppb)	49.6	40.0	110.2	36.1	9.2	18.6	6.3	1.2
Meteorological parameters								
RH (%)	58.1	55.9	35.7	70.4	49.3	30.3	27.8	81.9
T (°C)	28.2	26.7	32.9	26.7	-2.5	-2.9	0.3	-3.3
WS (m s^{-1})	0.5	0.7	0.5	0.3	1.5	2.6	1.0	0.6

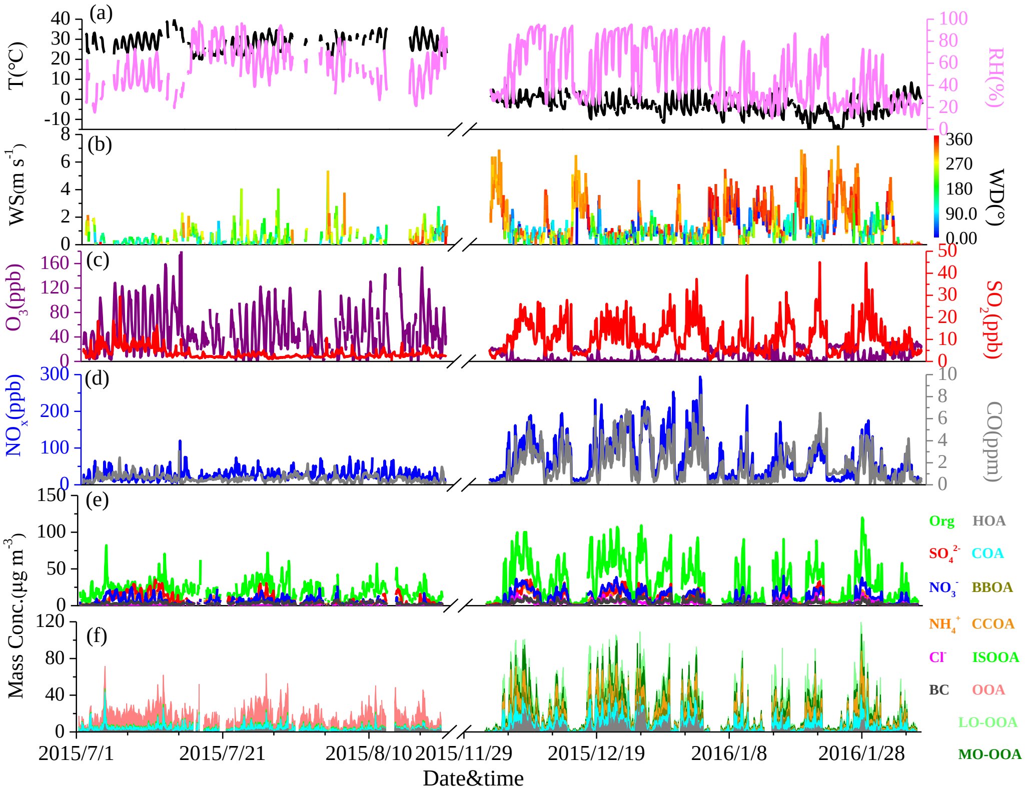

Figure 1. Time series of (a) temperature (T) and relative humidity (RH), (b) wind speed (WS) and wind direction (WD), (c) O_3 and SO_2, (d) CO and NO_x, (e) PM_1 species, (f) OA sources between summer and winter measurements.

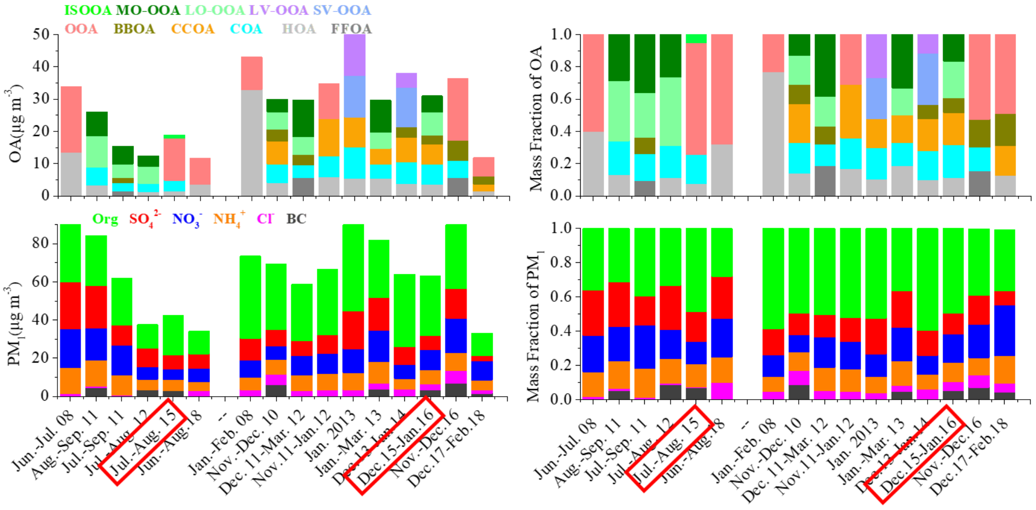

Figure 2. Summary of average chemical composition of OA and PM_1 in urban Beijing between summer and winter from 2008 to ~~2015~~2018. A more detailed description of the data is presented in Table S1. As for OA sources, fossil fuel related OA(FFOA) is the sum of HOA + CCOA, SV-OOA is semi-volatility OOA and LV-OOA is low-volatility OOA.

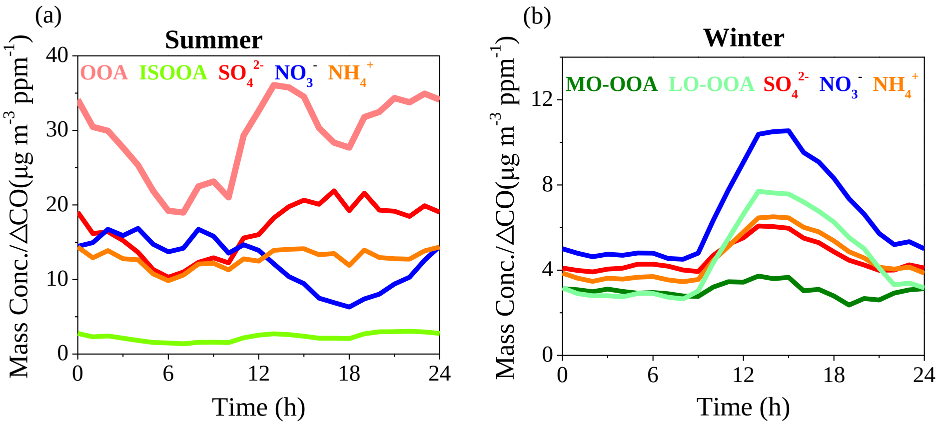

Figure 3. Average diurnal variations of secondary species/△CO during summer (a) and winter (b).

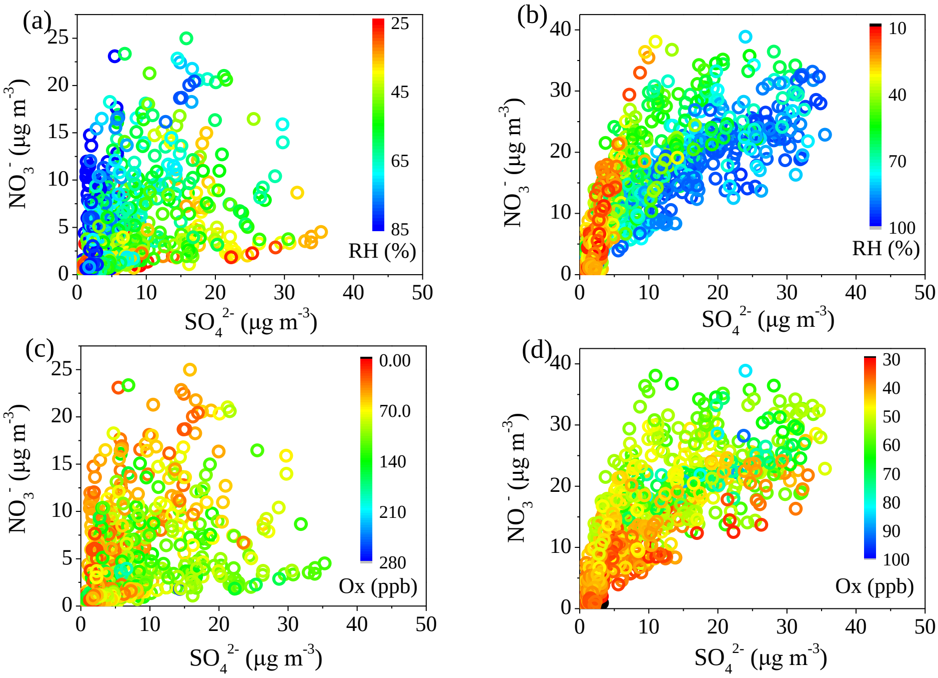

Figure 4. Correlations between NO_3^- and SO_4^{2-} color-coded with RH in summer (a) and winter (b), and correlations between NO_3^- and SO_4^{2-} color-coded with O_x concentration in summer (c) and winter (d).

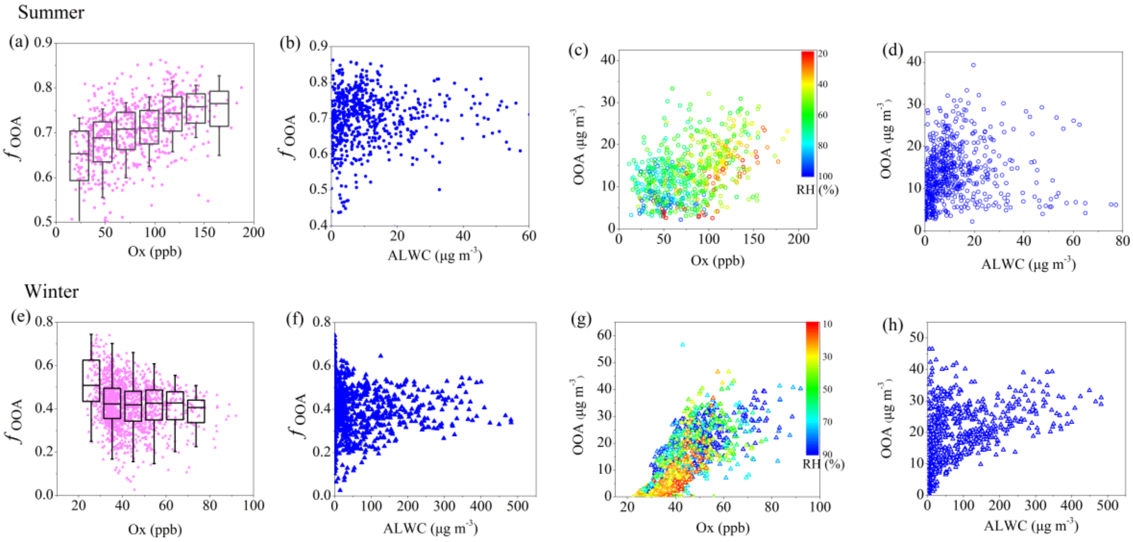

Figure 5. Scatterplots of f_{OOA} (mass fraction of OOA (related to OOA in summer and the total of LO-OOA+MO-OOA in winter) to OA) and mass concentration of OOA versus O_x and ALWC in summer (a, b, c, d) and winter (e, f, g, h).

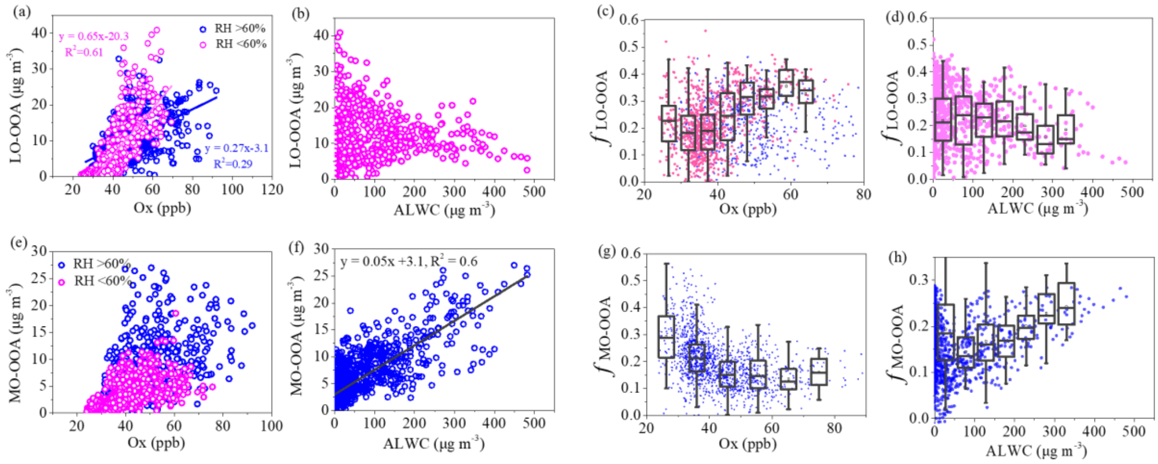

Figure 6. Relationship between LO-OOA or MO-OOA and O_x (a, e) and relationship between LO-OOA or MO-OOA and ALWC (b, f), as well as mass fractions of LO-OOA and MO-OOA as functions of Ox (c, g) and ALWC (d, h) in winter.

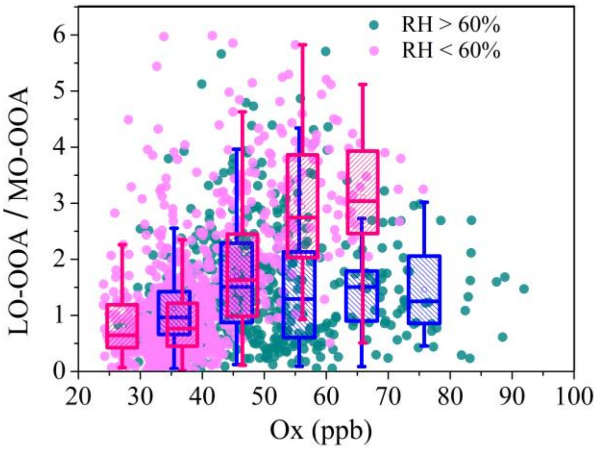

Figure 7. Scatterplots of LO-OOA/MO-OOA (mass ratio) versus O_x at RH > 60% and RH < 60% in winter.

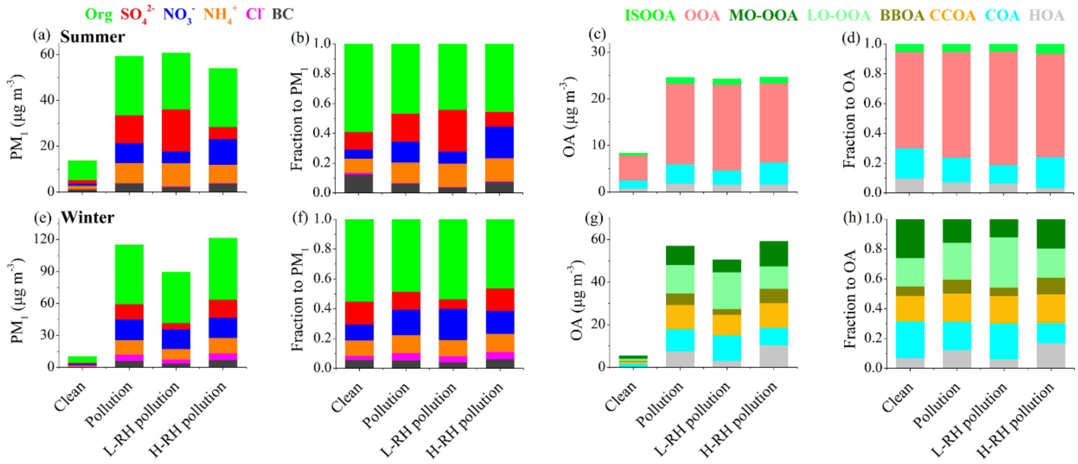

Figure 8. Mass concentrations and relative contributions of PM_1 species and OA sources during different periods in summer (a, b, c, d) and winter (e, f, g, h).

Supplement of:

Summertime and wintertime atmospheric processes of secondary aerosol in Beijing

Jing Duan[1,2,3], Ru-Jin Huang[1,2], Yongjie Li[4], Qi Chen[5], Yan Zheng[5], Yang Chen[6], Chunshui Lin[1,2], Haiyan Ni[1,2], Meng Wang[1,2], Jurgita Ovadnevaite[7], Darius Ceburnis[7], Chunying Chen[8], Douglas R. Worsnop[9], Thorsten Hoffmann[10], Colin O'Dowd[7], Junji Cao[1,2]

[1]State Key Laboratory of Loess and Quaternary Geology (SKLLQG) and Key Laboratory of Aerosol Chemistry & Physics (KLACP), Institute of Earth Environment, Chinese Academy of Sciences, Xi'an 710061, China

[2]CAS Center for Excellence in Quaternary Science and Global Change, Chinese Academy of Sciences, Xi'an 710061, China

[3]University of Chinese Academy of Sciences, Beijing 100049, China

[4]Department of Civil and Environmental Engineering, Faculty of Science and Technology, University of Macau, Taipa, Macau 999078, China

[5]State Key Joint Laboratory of Environmental Simulation and Pollution Control, College of Environmental Sciences and Engineering, Peking University, Beijing 100871, China

[6]Chongqing Institute of Green and Intelligent Technology, Chinese Academy of Sciences, Chongqing 400714, China

[7]School of Physics and Centre for Climate and Air Pollution Studies, Ryan Institute, National University of Ireland Galway, University Road, Galway, H91CF50, Ireland

[8]CAS Key Laboratory for Biological Effects of Nanomaterials and Nanosafety, National Centre for Nanoscience and Technology, Beijing 100191, China

[9]Aerodyne Research, Inc., Billerica, MA, USA

[10]Institute of Inorganic and Analytical Chemistry, Johannes Gutenberg University Mainz, Duesbergweg 10–14, Mainz 55128, Germany

Correspondence to: Ru-Jin Huang (rujin.huang@ieecas.cn) or Qi Chen (qichenpku@pku.edu.cn)

Section S1: Source apportionments for OA datasets

Separate OA source apportionments were conducted in summer and winter individually. According to the summer dataset, a range of solutions with three to five factors from unconstrained runs were first examined. As shown in Fig. S1, POA factors mixed seriously with SOA factors and identical source factors can't be resolved by PMF. There was a COA factor resolved in the 3-factor solution, while no clear HOA factor could be resolved and POA mixed seriously with SOA in factor 2, which may both contain HOA and OOA sources. No HOA could be resolved when increasing the factor numbers and the factor further split into non-meaningful profiles. Meanwhile, clear peaks in m/z 53 and m/z 82 were found in PMF solutions, indicating that there was likely have isoprene-derived sources mixed in POA or OOA factors, thus 4 factors were selected for the reasonable PMF solution. In order to get better results, the ME-2 approach was further applied to direct the apportionment towards an environmentally-meaningful solution by introducing *a priori* information (profiles) for certain factors. We constrained the COA and HOA using profiles from our previous study (Wang et al, 2017) and constrained ISOOA profile from Budisulistiorini et al. (2013). ~~To minimize the effect from non-local input profiles, the *a* value approach was used to adjust the input profiles to a certain extent.~~ To minimize the bias from non-local input profiles, the *a* value approach was used which determines the extent to which the output profiles can differ from the model inputs. It should be particularly noted that we used high *a* values of 0.3-0.6 to constrain the ISOOA profile, allowing large variation of the ISOOA output profile. To further evaluate the uncertainties of this factor, we performed ME-2 with each *a* value (0.3-0.6) for 20 times and calculated the standard deviation of these solutions, which is shown as the error bar in final ISOOA profile (Fig. S3). An uncertainty of ~20% was estimated for ISOOA in our measurement, suggesting a large uncertainty in ISOOA source in urban environment.

Similarly, a range of solutions with two to eight factors from unconstrained runs were first examined in winter. Fig. S2 showed the PMF results of 5-factor, 6-factor and 7-factor. POA factors including HOA, COA, BBOA and CCOA could be resolved in PMF solutions, while there was serious mixture between each other and POA with OOA. In order to get better results, the ME-2 approach was further applied to direct the apportionment towards an environmentally-meaningful solution by introducing *a priori* information (profiles) for certain factors. We constrained the HOA, COA, CCOA and BBOA using profiles from our previous study (Wang et al, 2017). Also, to minimize the effect from non-local input profiles (for all primary factors), the *a* value approach was used to adjust the input profiles to a certain extent.

Finally, we tested ME-2 solutions and selected reasonable results based on the verification of the rationality of unconstrained factors, distinct mass spectra and time series, interpretable diurnal cycles and good correlations with external tracers for all factors both in summer and winter. The final profiles and time series of individual factor were averaged from these reasonable solutions and the standard deviations of intensities at each *m/z* was shown as error bars in Fig. S3. Four OA factors including HOA, COA, ISOOA and OOA were resolved during summer, while six factors including HOA, COA, BBOA, CCOA, LO-OOA and MO-OOA were identified during winter.

Section S2: OA sources

Primary OA

HOA was resolved in both summer and winter, which was dominated by typical hydrocarbon ion series of C_nH_{2n+1} and C_nH_{2n-1}, particularly m/z 41, 43, 55, 57, 69 and 71 (Canagaratna et al., 2004; Mohr et al., 2009; Ng et al., 2011). The time series of HOA in summer and winter were both tightly correlated with that of BC ($R^2 = 0.62$ and 0.78 in summer and winter, respectively), which is a primary emission tracer of incomplete combustion. The diurnal cycles of HOA were characterized by high concentrations during nighttime (Fig. S4), likely due to increased diesel fleets which are allowed in urban Beijing only at night (Elser et al, 2016; Sun et al., 2016).

COA was also resolved in both summer and winter. The spectra of COA in our study were characterized by prominent ion peaks at *m/z* 55 and *m/z* 57 with higher m/z 55/57 ratio of 2.4 in summer and 2.1 in winter respectively, which have been shown to be robust markers for COA (Mohr et al., 2012; Crippa et al., 2013; Elser et al., 2016). Consistently, the time series of COA were correlated well with that of *m/z* 55 with R^2 = 0.72 and 0.66 during summer and winter respectively. Both the diurnal cycles of COA during summer and winter showed distinct peaks at lunch (12:00 LT) and dinner (20:00 LT) time.

BBOA and CCOA were only resolved in wintertime. The mass spectrum of BBOA showed prominent signals at m/z 60 ($C_2H_4O_2^+$) and 73 (95% of which is $C_3H_5O_2^+$), which are well known fragments of levoglucosan and mannosan produced from incomplete combustion and pyrolysis of cellulose and hemicelluloses from biomass burning (Alfarra et al., 2007; Lanz et al., 2007; Mohr et al., 2009). Consistently, the time series of BBOA correlated very well with that of m/z 60 (R^2 = 0.87). BBOA showed a clear diurnal cycle with higher concentration during nighttime than that in daytime. The mass spectrum of CCOA is characterized by prominent contributions of unsaturated hydrocarbons, particularly PAH-related ion peaks (e.g., 77, 91, and 115) (Dall'Osto et al., 2013; Hu et al., 2013). Strong correlation was found between the time series of CCOA and that of the external combustion tracer chloride with R^2 value of 0.73. Similar to BBOA, the mass concentration of CCOA during nighttime was much higher than that during daytime with the mass fraction increased from 10% in afternoon to 25% during night, further confirming the enhanced coal combustion emissions from domestic heating in wintertime nights.

Secondary OA

During summertime, an OOA factor dominated by high peak at m/z 44 (CO_2^+) with a f_{44}/f_{43} value of 3.2 was identified, The diurnal cycle of OOA showed an obvious peak in afternoon combined with the increasing mass fraction during the same period, and the time series of OOA correlated well with that of sulfate (R^2 = 0.6). Similar good correlations between OOA and sulfate were also observed in previous Beijing summer studies (Huang et al., 2010; Sun et al., 2010; Hu et al., 2016).

In addition to OOA, an ISOOA derived from isoprene-oxidation was resolved in summer Beijing. As shown in Fig.S3, the mass spectrum of ISOOA was characterized by distinct ion peaks at m/z 53 ($C_4H_5^+$) and m/z 82 ($C_5H_6O^+$), with correlation between the time series of ISOOA and m/z 82 (R^2 = 0.46). This ISOOA profile was consistent with that resolved from ACSM organic spectra based on field study during summertime in the southeastern US and demonstrated in lab chamber (Budisulistiorini et al., 2013; Hu et al., 2015; Xu et al., 2015). Meanwhile, the diurnal cycle of ISOOA displayed minor peaks in afternoon, likely due to the gas-phase photochemical processing during afternoon when temperature and photochemical activity are the highest in a day. Such diurnal behaviors are consistent with the T-dependence on isoprene photochemistry activities (Xu et al., 2015; Zhang et al., 2017).

In comparison, there was no ISOOA resolved during winter due to low temperature and less biogenic emission sources, whereas two secondary OA sources defined as LO-OOA and MO-OOA were identified. As shown in Fig. S3, LO-OOA and MO-OOA both showed high ratios of intensity at m/z 44 over that at m/z 43 in mass spectra (the $f_{44}/_{43}$ value of MO-OOA (8.6) was much higher than that of LO-OOA (2.61)). However, their time series and diurnal cycles differed from each other greatly. The time series of LO-OOA was highly correlated with that of nitrate in the entire winter period with $R^2 = 0.80$, while the time series of MO-OOA had a good correlation ($R^2 = 0.71$) with that of sulfate. The diurnal cycles of LO-OOA showed a dominant increasing trend from 8:00 to 20:00 LT, meanwhile the mass fraction of LO-OOA increased during the same period in daytime, which was similar with that of nitrate (As shown in Fig. S4). In comparison, the diurnal cycles of both concentration and fraction of MO-OOA showed decreasing trend from 8:00 LT to 16:00 LT, which was consistent with that of sulfate and RH.

Section S3: Diurnal cycles of PM_1 species

The diurnal cycles of PM_1 species between summer and winter are shown in Fig. S4. OA was characterized by two peaks occurring around noon (12:00-13:00 LT) and the evening (19:00-22:00 LT) both in summer and winter. The peak in noon was larger in summer than that in winter, likely due to the stronger photochemical oxidation capacity in daytime during summer. The diurnal cycle of mass fraction of OA in summer was also more variable than that in winter with two obvious peaks in the noon and evening. BC and chloride also showed similar diurnal cycles in summer and winter because both are primary emissions, and their concentrations were much higher during night than during day in winter because enhanced emissions from residential heating activities. Compared to primary species, secondary species displayed largely different diurnal cycles between summer and winter. In summer, sulfate showed continuous increase from 8:00 LT to 17:00 LT, even in the afternoon at the highest planetary boundary layer height as reflected in the trough of OA, suggesting its efficient formation. However, there was no similar increasing peak in winter, yet decreased from 8:00 LT to 16:00 LT instead and higher concentration in nighttime than daytime was observed during winter. In comparison, nitrate showed contrary diurnal cycles with that of sulfate both in summer and winter. The diurnal cycle of nitrate displayed a peak in the morning and then decreased dramatically from 8:00 LT to 16:00 LT during summer, while increasing trend of nitrate during the same time (8:00-16:00 LT) was observed in winter. Consistently, dominant increase of the mass fraction of sulfate in afternoon was observed in summer while similar increase was found for nitrate fraction in winter. Associated with sulfate and nitrate, the diurnal cycles of ammonium were affected by both sulfate and nitrate formation mechanisms, which showed medium increasing trends in daytime both in summer and winter.

Table S1. A summary of submicron aerosol composition and OA factors from AMS/ACSM measurements in Beijing, China.

Season	Summer						Winter									
Date	Jun-Jul, 2008	Aug- Sep, 2011	Jul-Sep, 2011	Jul–Aug, 2012	Jul-Aug, 2015	Jun-Aug, 2018	Jan-Feb, 2008	Nov-Dec, 2010	Dec, 2011-Mar, 2012	Nov, 2011-Jan, 2012	Jan, 2013	Jan–Mar, 2013	Dec, 2013-Jan, 2014	Dec, 2015 - Feb, 2016	Nov-Dec,2016	Dec,17-Feb,18
Ref.	Zhang et al., 2013	Hu et al., 2016	Sun et al., 2015, 2018	Hu et al., 2017	This study	Zhou et al., 2019	Zhang et al., 2013	Hu et al., 2016	Sun et al., 2015, 2018	Sun et al., 2013	Zhang et al., 2014	Hu et al., 2017	Sun et al., 2016	This study	Xu et al.,2018	Li et al., 2019
PM_1	94.0	77.9	61.6	37.6	41.0	31.0	73.5	69.5	58.7	66.8	94.0	81.7	64.1	63.2	92.9	33.2
SO_4^{2-}	24.8	22	10.6	9.7	7.5	7.6	11.4	8.7	7.7	9.4	19.6	17.4	9.4	7.6	15.5	2.8
NO_3^-	20.1	16.8	15.6	6.4	5.6	7.0	9.2	6.8	10.3	10.7	12.5	16.2	7.2	10.5	18.1	9.9
NH_4^+	13.7	13.7	10.5	5.4	5.7	4.7	6.4	7.7	8.1	8.7	8.9	11.7	5.4	7.4	9.5	5.4
Cl^-	1.56	1.0	0.8	0.4	0.2	3.1	3.5	5.8	3.0	3.3	3.6	2.8	4.0	3.1	6.7	1.7
BC	-	4.4	-	3.2	2.9	-	-	6.0	-	-	-	3.9	-	3.4	6.7	1.5
FFOA	-	-	1.45	-	-	-	-	-	5.6	-	-	-	-	-	5.6	-
HOA	13.5	3.4	-	1.4	1.5	3.7	33	4.2	-	5.9	5.4	5.5	3.9	3.6	-	1.5
COA	-	5.5	2.6	2.5	3.4	-	-	5.7	4.0	6.6	9.8	4.3	6.7	6.3	5.4	-
CCOA	-	-	-	-	-	-	-	7.2	-	11.4	9.3	5.0	7.6	6.1	-	2.2
BBOA	-	-	1.55	-	-	-	-	3.6	3.2	-	-	-	2.2	2.8	6.3	2.4
SV-OOA	-	-	-	-	-	-	-	-	-	-	12.8	-	12.1	-	-	-
LV-OOA	-	-	-	-	-	-	-	-	-	-	13.8	-	4.4	-	-	-
LO-OOA	-	9.7	4.3	5.3	-	-	-	5.4	5.5	-	-	5.0	-	7.1	-	-
MO-OOA	-	7.4	5.6	3.3	-	-	-	3.9	11.4	-	-	9.8	-	5.1	-	-
OOA	20.3	-	-	-	13.0	8.1	10	-	-	10.8	-	-	-	-	19	5.8
ISOOA	-	-	-	-	1.0	-	-	-	-	-	-	-	-	-	-	-

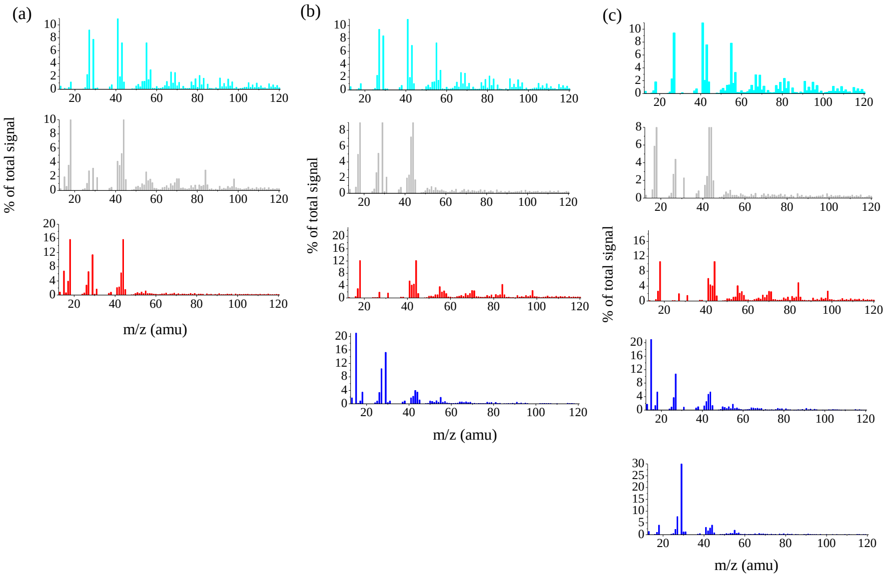

Figure S1. PMF profiles of OA sources for 3, 4 and 5 factor solutions during summer.

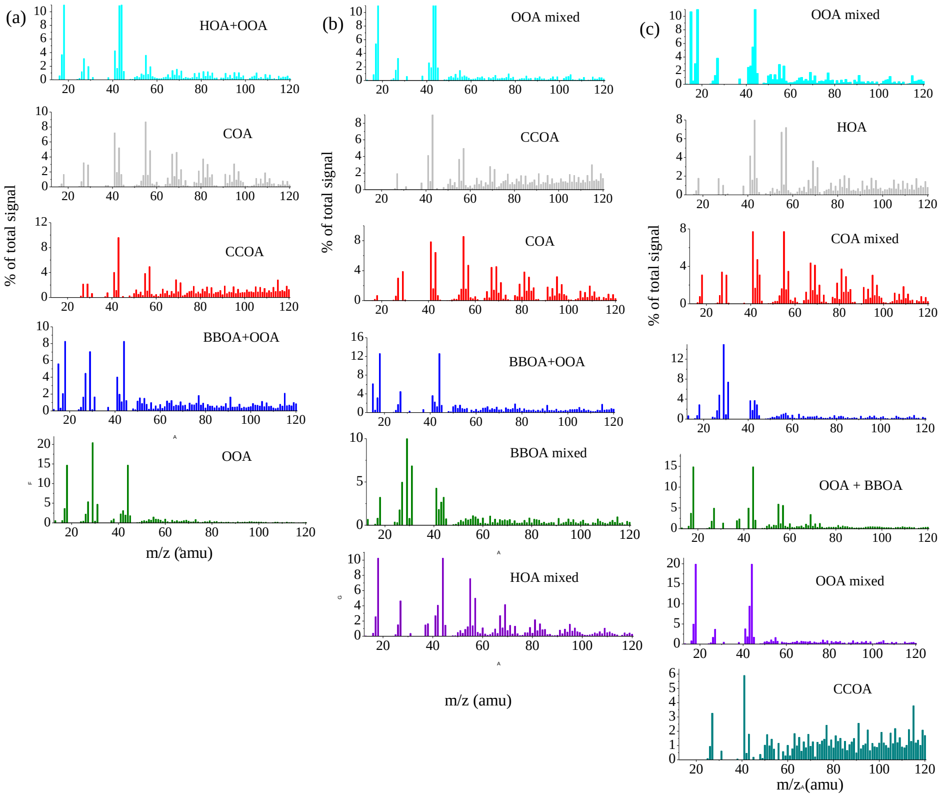

Figure S2. PMF profiles of OA sources for 5, 6 and 7 factor solutions during winter.

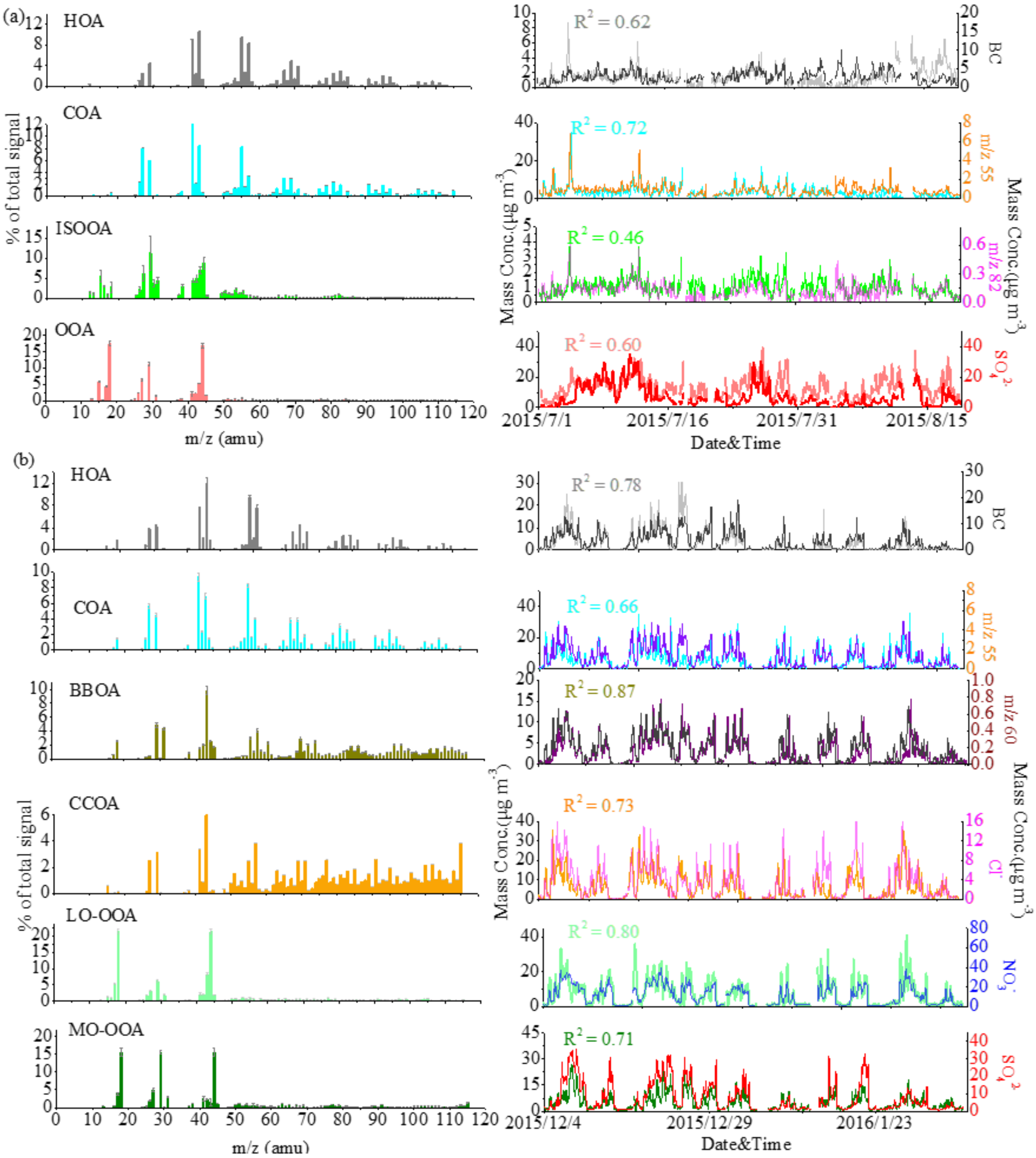

Figure S3. Mass spectrums (left) and time series (right) of OA sources during summer (a) and winter (b). Error bars of mass spectrums represent the standard deviation of each m/z over all accepted solutions.

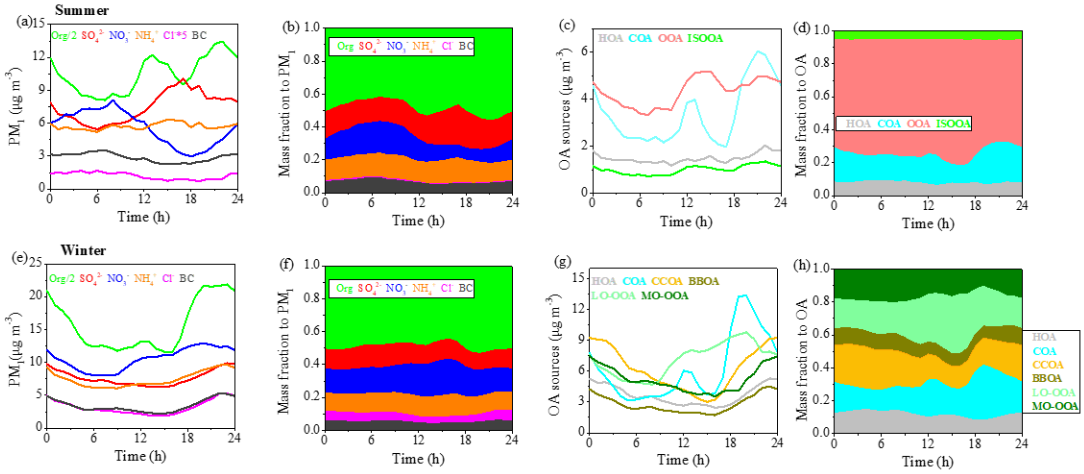

Figure S4. Diurnal variations of mass concentrations and mass fractions of PM$_1$ components and OA sources during summer (a, b, c, d) and winter (e, f, g, h).

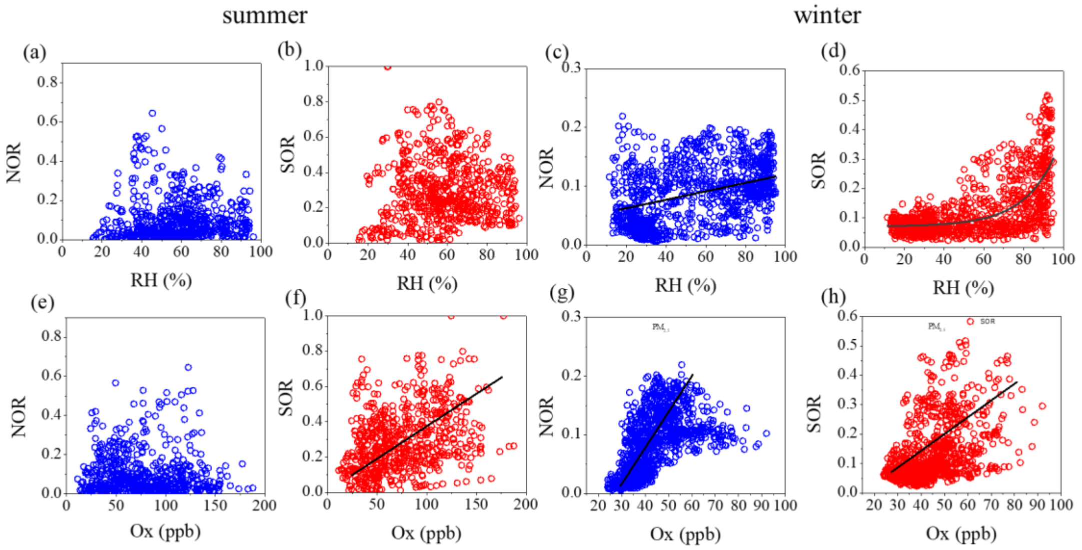

Figure S5. Effects of RH on NOR or SOR during summer (a, b) and winter (c, d), as well as effects of Ox on NOR or SOR during summer (e, f) and winter (g, h).

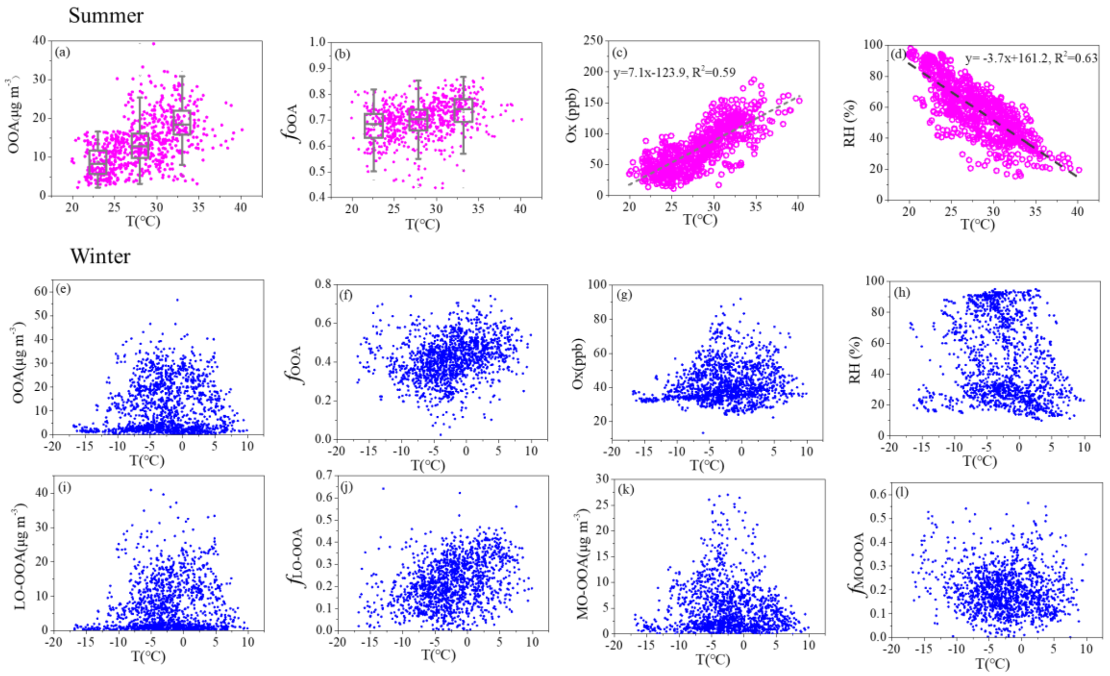

Figure S6. Effects of temperature on the formation of OOA in summer (a-d) and winter (e-l). OOA in winter refers to the total of LO-OOA and MO-OOA.

Reference:

Alfarra, M. R., Prévôt, A. S. H., Szidat, S., Sandradewi, J., Weimer, S., Schreiber, D., Mohr, M., and Baltensperger, U.: Identification of the mass spectral signature of organic aerosols from wood burning emissions, Environ. Sci. Technol., 41(16), 5770–5777, 2007.

Budisulistiorini, S. H., Canagaratna, M. R., Croteau, P. L., Marth, W. J., Baumann, K., Edgerton, E. S., Shaw, S. L., Knipping, E. M., Worsnop, D. R., Jayne, J. T., Gold, A., and Surratt, J. D.: Real-time continuous characterization of secondary organic aerosol derived from isoprene epoxydiols in downtown Atlanta, Georgia, using the Aerodyne Aerosol Chemical Speciation Monitor, Environ. Sci. Technol., 47(11), 5686–5694, 2013.

Canagaratna, M. R., Jayne, J. T., Ghertner, D. A., Herndon, S., Shi, Q., Jimenez, J. L., Silva, P. J., Williams, P., Lanni, T., Drewnick, F., Demerjian, K. L., Kolb, C. E., and Worsnop, D. R.: Chase studies of particulate emissions from in-use New York City vehicles, Aerosol Sci. Tech., 38, 555–573, 2004.

Crippa, M., Decarlo, P. F., Slowik, J. G., Mohr, C., Heringa, M. F., Chirico, R., Poulain, L., Freutel, F., Sciare, J., Cozic, J., Di Marco, C. F., Elsasser, M., Nicolas, J., Marchand, Nicolas, Abidi, E., Wiedensohler, A., Drewnick, F., Schneider, J., Borrmann, S., Nemitz, E., Zimmermann, R., Jaffrezo, J.-L., Prévôt, A. S. H., and Baltensperger U.: Wintertime aerosol chemical composition and source apportionment of the organic fraction in the metropolitan area of Paris, Atmos. Chem. Phys., 13, 961–981, https://doi.org/10.5194/acp-13-961-2013, 2013.

Dall'Osto, M., Ovadnevaite, J., Ceburnis, D., Martin, D., Healy, R. M., O'Connor, I. P., Kourtchev, I., Sodeau, J. R., Wenger, J. C., and O'Dowd, C.: Characterization of urban aerosol in Cork city (Ireland) using aerosol mass spectrometry, Atmos. Chem. Phys., 13, 4997–5015, https://doi.org/10.5194/acp-13-4997-2013, 2013.

Elser, M., Huang, R. J., Wolf, R., Slowik, J. G., Wang, Q., Canonaco, F., Li, G., Bozzetti, C., Daellenbach, K. R., Huang, Y., Zhang, R., Li, Z., Cao, J., Baltensperger, U., El-Haddad, I., and Prévôt, A. S. H.: New insights into PM2.5 chemical composition and sources in two major cities in China during extreme haze events using aerosol mass spectrometry, Atmos. Chem. Phys., 16, 3207–3225, https://doi.org/10.5194/acp-16-3207-2016, 2016.

Hu, W. W., Hu, M., Yuan, B., Jimenez, J. L., Tang, Q., Peng, J. F., Hu, W., Shao, M., Wang, M., Zheng, L. M., Wu, Y. S., Gong, Z. H., Huang, X. F., and He, L. Y.: Insights on organic aerosol aging and the influence of coal combustion at a regional receptor site of central eastern China, Atmos. Chem. Phys., 13, 10095–10112, https://doi.org/10.5194/acp-13-10095-2013, 2013.

Hu, W. W., Campuzano-Jost, P., Palm, B. B., Day, D. A., Ortega, A. M., Hayes, P. L., Krechmer, J. E., Chen, Q., Kuwata, M., Liu, Y. J., de Sá, S. S., McKinney, K., Martin, S. T., Hu, M., Budisulistiorini, S. H., Riva, M., Surratt, J. D., St. Clair, J. M., Isaacman-Van Wertz, G., Yee, L. D., Goldstein, A. H., Carbone, S., Brito, J., Artaxo, P., de Gouw, J. A., Koss, A., Wisthaler, A., Mikoviny, T., Karl, T., Kaser, L., Jud, W., Hansel, A., Docherty, K. S., Alexander, M. L., Robinson, N. H., Coe, H., Allan, J. D., Canagaratna, M. R., Paulot, F., and Jimenez, J. L.: Characterization of a real-time tracer for isoprene epoxydiols-derived secondary organic aerosol (IEPOX-SOA) from aerosol mass spectrometer measurements, Atmos. Chem. Phys., 15, 11807–11833, https://doi.org/10.5194/acp-15-11807-2015, 2015.

Hu, W., Hu, M., Hu, W., Jimenez, J. L., Yuan, B., Chen, W., Wang, M., Wu, Y., Chen, C., Wang, Z., Peng, J., Zeng, L., and Shao, M.: Chemical composition, sources, and aging process of submicron aerosols in Beijing: Contrast between summer and winter, J. Geophys. Res. Atmos., 121(4), 1955–1977, https://doi.org/10.1002/2015JD024020, 2016.

Hu, W., Hu, M., Hu, W.-W., Zheng, J., Chen, C., Wu, Y., and Guo, S.: Seasonal variations in high time-resolved chemical compositions, sources, and evolution of atmospheric submicron aerosols in the megacity Beijing, Atmos. Chem. Phys., 17, 9979–10000, https://doi.org/10.5194/acp-17-9979-2017, 2017.

Huang, X. F., He, L. Y., Hu, M., Canagaratna, M. R., Sun, Y., Zhang, Q., Zhu, T., Xue, L., Zeng, L. W., Liu, X. G., Zhang, Y. H., Jayne, J. T., Ng, N. L., and Worsnop, D. R.: Highly time-resolved chemical characterization of atmospheric submicron particles during 2008 Beijing Olympic Games using an Aerodyne High-Resolution Aerosol Mass Spectrometer, Atmos. Chem. Phys., 10, 8933–8945, https://doi.org/10.5194/acp-10-8933-2010, 2010.

Lanz, V. A., Alfarra, M. R., Baltensperger, U., Buchmann, B., Hueglin, C., and Prévôt, A. S. H.: Source apportionment of submicron organic aerosols at an urban site by factor analytical modelling of aerosol mass spectra, Atmos. Chem. Phys., 7, 1503–1522, https://doi.org/10.5194/acp-7-1503-2007, 2007.

Li, H., Cheng, J., Zhang, Q., Zheng, B., Zhang, Y., Zheng, G., and He, K.: Rapid transition in winter aerosol composition in Beijing from 2014 to 2017: response to clean air actions, Atmos. Chem. Phys., 19, 11485–11499, https://doi.org/10.5194/acp-19-11485-2019, 2019.

Mohr, C., Huffman, J. A., Cubison, M. J., Aiken, A. C., Docherty, K. S., Kimmel, J. R., Ulbrich, I. M., Hannigan, M., and Jimenez, J. L.: Characterization of primary organic aerosol emissions from meat cooking, trash burning, and motor vehicles with High-Resolution Aerosol Mass Spectrometry and comparison with ambient and chamber observations, Environ. Sci. Technol., 43, 2443–2449, 2009.

Mohr, C., DeCarlo, P. F., Heringa, M. F., Chirico, R., Slowik, J. G., Richter, R., Reche, C., Alastuey, A., Querol, X., Seco, R., Peñuelas, J., Jiménez, J. L., Crippa, M., Zimmermann, R., Baltensperger, U., and Prévôt, A. S. H.: Identification and quantification of organic aerosol from cooking and other sources in Barcelona using aerosol mass spectrometer data, Atmos. Chem. Phys., 12, 1649–1665, https://doi.org/10.5194/acp-12-1649-2012, 2012.

Ng, N. L., Canagaratna, M. R., Jimenez, J. L., Zhang, Q., Ulbrich, M., and Worsnop, D. R.: Real-time methods for estimating organic component mass concentrations from aerosol mass spectrometer data, Environ. Sci. Technol., 45, 910–916, https://doi.org/10.1021 /es102951k, 2011.

Sun, J., Zhang, Q., Canagaratna, M. R., Zhang, Y., Ng, N. L., Sun, Y., Jayne, J. T., Zhang, X., Zhang, X., and Worsnop, D. R.: Highly time- and size-resolved characterization of submicron aerosol particles in Beijing using an Aerodyne Aerosol Mass Spectrometer, Atmos. Environ., 44, 131–140, https://doi.org/10.1016/j.atmosenv.2009.03.020, 2010.

Sun, Y. L., Wang, Z. F., Fu, P. Q., Yang, T., Jiang, Q., Dong, H. B., Li, J., and Jia, J. J.: Aerosol composition, sources and processes during wintertime in Beijing, China, Atmos. Chem. Phys., 13, 4577–4592, https://doi.org/10.5194/acp-13-4577-2013, 2013.

Sun, Y. L., Wang, Z. F., Du, W., Zhang, Q., Wang, Q. Q., Fu, P. Q., Pan, X., Li, J., Jayne, J., and Worsnop, D. R.: Long-term real-time measurements of aerosol particle composition in Beijing, China: seasonal variations, meteorological effects, and source analysis, Atmos. Chem. Phys., 15, 10149–10165, https://doi.org/10.5194/acp-15-10149-2015, 2015.

Sun, Y., Du, W., Fu, P., Wang, Q., Li, J., Ge, X., Zhang, Q., Zhu, C., Ren, L., Xu, W., Zhao, J., Han, T., Worsnop, D. R., and Wang, Z.: Primary and secondary aerosols in Beijing in winter: sources, variations and processes, Atmos. Chem. Phys., 16, 8309–8329, https://doi.org/10.5194/acp-16-8309-2016, 2016.

Sun, Y., Xu, W., Zhang, Q., Jiang, Q., Canonaco, F., Prévôt, A. S., Fu, P., Li, J., Jayne, J., Worsnop, D. R., and Wang, Z.: Source apportionment of organic aerosol from two-year highly time-resolved measurements by an aerosol chemical speciation monitor in Beijing, China, Atmos. Chem. Phys., 18(12), 8469–8489, 2018.

Wang, Y. C., Huang, R. J., Ni, H. Y., Chen, Y., Wang, Q. Y., Li, G. H., Tie, X. X., Shen, Z. X., Huang, Y., Liu, S. X., Dong, W. M., Xue, P., Fröhlich, R., Canonaco, F., Elser, M., Daellenbach, K.R., Bozzetti, C., Haddad, EI., and Cao, J. J.: Chemical composition, sources and secondary processes of aerosols in Baoji city of northwest China, Atmos. Environ., 158, 128–137, https://doi.org/10.1016/j.atmosenv.2017.03.026, 2017.

Xu, L., Guo, H., Boyd, C. M., Klein, M., Bougiatioti, A., Cerully, K. M., Hite, J. R., Isaacman-VanWertz, G., Kreisberg, N. M., Knote, C., Olson, K., Koss, A., Goldstein, A. H., Hering, S. V., de Gouw, J., Baumann, K., Lee, S. H., Nenes, A., Weber, R. J., and Ng, N.L.: Effects of anthropogenic emissions on aerosol formation from isoprene and monoterpenes in the southeastern United States, Proc. Natl. Acad. Sci. U.S.A., 112(32), E4506–E4507, 2015.

Xu, W. Q., Sun, Y. L., Wang, Q. Q., Zhao, J., Wang, J. F., Ge, X. L., Xie, C. H., Zhou, W., Du, W., Li, J., Fu, P. Q., Wang, Z. F., Worsnop, D. R., and Coe, H.: Changes in aerosol chemistry from 2014 to 2016 in winter in Beijing: insights from high resolution aerosol mass spectrometry, J. Geophys. Res. Atmos., 124(2), 1132–1147, 2018.

Zhang, J. K., Sun, Y., Liu, Z. R., Ji, D. S., Hu, B., Liu, Q., and Wang, Y. S.: Characterization of submicron aerosols during a month of serious pollution in Beijing, 2013, Atmos. Chem. Phys., 14, 2887-2903, https://doi.org/10.5194/acp-14-2887-2014, 2014.

Zhang, Y., Sun, J., Zhang, X., Shen, X., Wang, T., and Qin, M.: Seasonal characterization of components and size distributions for submicron aerosols in Beijing, Sci. China Earth Sci., 56, 890–900, https://doi.org/10.1007/s11430-012-4515-z, 2013.

Zhang, Y. J., Tang, L. L., Sun, Y. L., Favez, O., Canonaco, F., Albinet, A., Couvidat, F., Liu, D. T., Jayne, J. T., Wang, Z., Croteau, P. L., Canagaratna, M. R., Zhou, H. C., Prevot, A. S. H., and Worsnop, D.R.: Limited formation of isoprene epoxydiols-derived secondary organic aerosol under NOx-rich environments in Eastern China, Geophys. Res. Lett., 44(4), 2035–2043, https://doi.org/10.1002/2016GL072368, 2017.

Zhou, W., Gao, M., He, Y., Wang, Q., Xie, C., Xu, W., Zhao, J., Du, W., Qiu, Y., Lei, L., Fu, P., Wang, Z., Worsnop, D.R., Zhang, Q., and Sun, Y.: Response of aerosol chemistry to clean air action in Beijing, China: Insights from two-year ACSM measurements and model simulations, Environ. Pollut., 255, 113345, 2019.